5-2012

Heterogeneous Deformation of Gabbroic Rocks

Calvin Mako
calvin.mako@umit.maine.edu

HETEROGENEOUS DEFORMATION OF GABBROIC ROCKS CENTRAL METASEDIMENTARY BELT BOUNDARY THRUST ZONE GRENVILLE PROVINCE CANADA

by

Calvin Mako

A Thesis Submitted in Partial Fulfillment
of the Requirements for a Degree with Honors
(Earth Science)

The Honors College

University of Maine

May 2012

Advisory Committee:

Christopher Gerbi, Assistant Professor of Earth Sciences, Advisor
Scott Johnson, Professor of Earth Sciences and Department Chair
Peter Koons, Professor of Earth Sciences
Martin Yates, Lab Manager and Associate Scientist in Earth Sciences
Melissa Ladenheim, Adjunct Assistant Professor in Honors (Folklore)

Abstract

The Grenville province is the exhumed remains of a more than 1 billion year old orogen. Mid to lower crustal rocks of this orogen are now exposed at the surface, affording the opportunity to examine deeper crustal processes during orogeny. I have studied an outcrop of anorthositic gabbro from the Central Metasedimentary Belt boundary thrust zone (CMBbtz) in the Grenville province of southern Ontario. The CMBbtz is a region that separates two major lithotectonic domains of this part of the Grenville province and is thought to have accommodated large scale thrusting in the mesoproterozoic era. The CMBbtz comprises large crystalline thrust sheets in a marble tectonic breccia and many anastomosing ductile shear zones. My outcrop occurs in the newly proposed Salerno Creek deformation zone which is thought be a major shear zone of the CMBbtz.

I have examined an outcrop that exhibits meter-scale shear zones and ductile strain localization. I have documented textural, chemical and microstructural characteristics across the varying degrees of strain. Based on these observations, I have proposed mechanisms by which these rocks have become locally weak, allowing strain to localize. The two primary minerals in these rocks, hornblende and plagioclase, appear to have deformed primarily by brittle fracturing and subgrain rotation recrystallization, respectively. Possible mechanisms of shear zone localization include original heterogeneities in the outcrop, the introduction of fluids and stress concentration in cross-cutting veins. There are many complex factors controlling these latter two mechanisms.

Ad Majorem Dei Gloriam

ACKNOWLEDGEMENTS

There are several people that I would like to thank for their help and support while I have worked on this thesis and throughout my college career. Without guidance from these people I would not be the student or person that I am today. First, I thank my advisor, Chris Gerbi, for tremendous intellectual help and patience over the course of my research. I thank my thesis committee members, Marty Yates, Scott Johnson, Peter Koons and Melissa Ladenheim who have also provided much needed advice and have also taught me a great deal in my course work at UMaine. Also, I am greatly indebted to graduate students Deb Shulman, Ben Frieman, Nancy Price and JohnRyan MacGregor for their generous assistance with my thesis work. I am also very grateful to the Keck Geology Consortium for the learning experiences it provided and for the friendships I have made in my Keck experience. Many thanks go out to my Keck advisors, Michelle Markley, William Peck and Steve Dunn.

I must also thank my parents for their love, encouragement and the extraordinary opportunities they have provided for me; I would be nothing without them. For spiritual guidance and friendship, I would like to thank Father Bill Labbe. For love, support and joy, I would like to thank Alyssa McCluskey. I also thank the University of Maine. It is a truly great place. I have made irreplaceable friends, learned invaluable lessons and made timeless memories all because of this university.

TABLE OF CONTENTS

LIST OF FIGURES

LIST OF TABLES

INTRODUCTION

Differential stresses of varying magnitudes are pervasive within the crust and lithosphere and result from the density-gravity driven tectonic forces that are pervasive in these regions. In the middle to lower crust, deformation arising from these stresses is usually ductile and in the upper crust it is generally brittle (Davis and Reynolds, 1996). In many cases deformation and strain are localized to discrete shear zones rather than being distributed throughout the crust (Montesi and Zuber 2002). This behavior controls the outcome of many episodes of stress on the Earth and produces many structures that are observable in nature such as faults, mountains and plate boundaries. The study of strain localization is thus essential for our understanding of many of the features that we see on Earth.

Localization results from existing and evolving strength heterogeneities which allow strain to be more easily accommodated in certain areas. The weaker a rock is, the less stress must be applied to produce a given strain rate. Thus, if a body of rock is weaker in a discrete area, strain will be taken up more easily in that area and localized deformation can occur. Similarly, if local weaknesses are introduced into a rock by some process strain localization can take place (Davis and Reynolds, 1996). The means by which rocks are inherently weak or become weak exert a primary control on strain localization. Thus, understanding rock weakening is of central importance to the study of strain localization (Manchtelow and Pennacchioni 2005).

The purpose of this study is to examine an outcrop where strain localization occurs and document the differences in various characteristics between strained and

unstrained material there. From the data I have collected I will suggest what has made these rocks initially weak or mechanisms by which these rocks have become weaker, localizing strain. Using electron backscatter diffraction (EBSD), wavelength dispersive spectroscopy (WDS) and optical microscopy, I have documented characteristics of low to high strain rocks that give clues to the mechanisms of strain localization.

The rocks of interest are taken from the Grenville province in southern Ontario, Canada which is an ancient orogen that was active between 1.4 and 1.0 billion years ago. In this location, upper amphibolite facies rocks from the middle to lower crust have been exhumed by erosion and brought to the surface. The outcrop that I have sampled is an expression of the Salerno Creek deformation zone, a newly described mylonite zone in the upper part of the Central Metasedimentary Belt boundary thrust zone (CMBbtz) (Easton and Kamo 2011). The CMBbtz is a zone of significant thrusting between two major lithotectonic domains of the Grenville province (Carr et al 2000).

This outcrop exhibits strain localization on a small scale. Over the space of about 25 meters rocks are variably strained, ranging from almost completely unstrained to apparently highly strained. This is a natural example that provides the opportunity to study how these rocks have become locally weak or what inherent weaknesses exist in these rocks. This study will add to the larger body of data relating to strain localization and provide insight into the processes that have acted in this outcrop.

BACKGROUND

1. The Grenville Province

Grenville related rocks are thought to run from Texas to northern Canada (McLelland et al. 2010) but our primary interest lies in southern Ontario (Figure 1). Here, the Grenville province comprises upper amphibolite to granulite facies metamorphic rocks that are interpreted as part of an ancient, mesoproterozoic orogenic belt (Easton 2000). This region provides opportunities to constrain the tectonic history of the Grenville orogeny with implications for the larger picture of proterozoic tectonics (Hanmer et al. 2000). In southern Ontario, mid to deep crustal Grenville rocks are exposed at the surface after almost a billion years of exhumation. This view allows us to examine the processes that were at work in the active Grenville orogen, including strain localization. This is particularly useful because deep crustal rocks from currently active orogens are not directly available for study.

The rocks of the Grenville province are thought to have come to their current state over a long period of convergent tectonics interspersed with short periods of extension, from 1.4 to 1.0 billion years ago (Carr et al. 2000). Over this period a number of different events are distinguishable, relating to the accretion of island arcs and continental blocks to the Laurentian (pre-North American) margin. There is widespread disagreement in the literature as to the nature and timing of these events (Hanmer et al. 2000). However, the end result of this convergence is generally thought to have been the collision of the Amazonian (pre-South American) continent with Laurentia close to 1.0

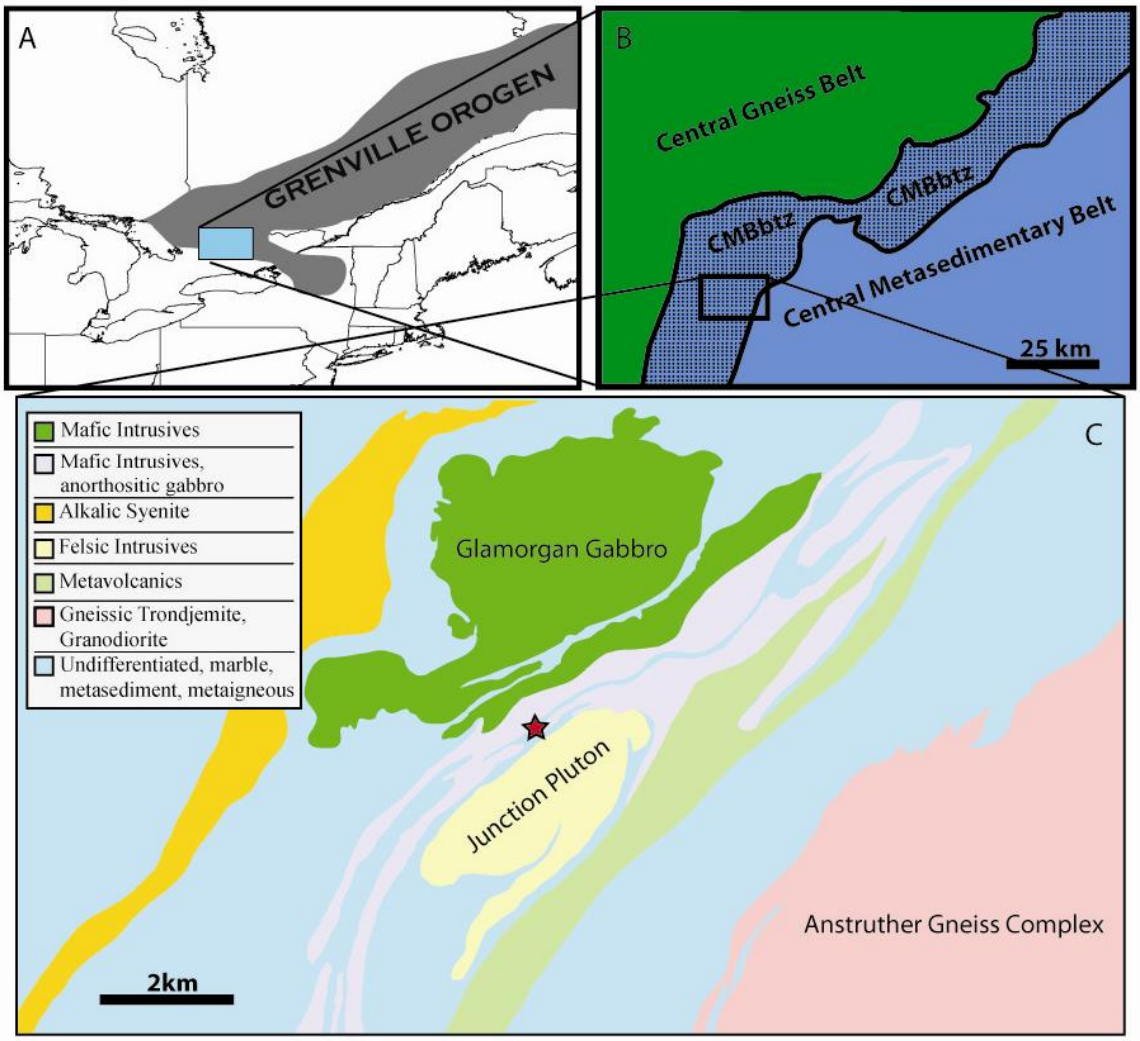

Figure 1. A) View of the larger Canadian Grenville pronvince. B) Closerview of the CMB and CGB with the CMBbtz in between (stippled area). (Boundaries drawn after Map 2544, Ontario Ministry of Northern Development and Mines, Bedrock Geology of Ontario: Southern Sheet.) C) Map view of local geologic units. The outcrop location with a star marking the outcrop location. The area is dominated by metaigneous thrust sheets and bodies in a marble breccia matrix. (Boundaries drawn after Lumbers and Vertolli 2000, Map P.3405, Ontario Geologic survey, Precambrain Geology, Gooderham area.)

Ga (McLelland et al. 2010) with smaller terranes caught in between. High grade metamorphism and ductile thrusting events were common throughout this history.

The Grenville province in southern Ontario can be divided into several lithotectonic domains including the central gneiss belt (CGB) and the central metasedimentary belt (CMB, sometimes referred to as the composite arc belt) (Figure 1). The CGB to the northwest is thought to be the reworked margin of the Laurentian continent and consists primarily of gneissic metaigneous rocks (Wodicka et al. 2000). The CMB comprises metasedimentary and metaigneous rocks including marbles, gabbros, granites and metavolcanics. It is interpreted to be the remnants of island arcs and possibly a back arc basin (Hanmer et al. 2000). Temperature and pressure of metamorphism estimates have ranged from 550˚C to 750˚C and 5-7 kbar respectively for this area (Montanye 2012, Nesbit 2012, Gerace-Fowler 2012, Easton 2000). These domains are separated by the central metasedimentary belt boundary thrust zone (CMBbtz), which is lithologically similar to the CMB but seems to have been more deformed and is interpreted as a major crustal-scale shear zone (McEachern and VanBreeman 1993).

The CMBbtz consists of many crystalline thrust sheets, surrounded by an anastomosing network of ductile shear zones (Hanmer and McEachern 1992). Marble tectonic breccia is a common feature with clasts ranging from centimeter to kilometer scale. This zone is thought to have accommodated significant northwest directed thrusting in two major episodes, the first of which occurred about 1.2 Ga and is thought to mark the closing of a back arc basin on the Laurentian margin (McEarchern and VanBreeman 1993). The second event was a reactivation of the zone at around 1.1 Ga

(Timmerman et al. 1997) which may have resulted from the collision of Amazonia with Laurentia (McEarchern and VanBreeman 1993). Hanmer and McEachern (1992) proposed that the base of the CMB and crustal scale thrusting may have been localized by a string of discontinuous rigid gabbroic bodies along the length of the CMB hanging wall, though there has been some debate about this point (Miller and Lentz 1993). This outcrop of gabbro which I have studied can be included in this string of gabbro, so it may have had significance in localizing the CMBbtz.

Among the many shear zones of the CMBbtz, Easton and Kamo (2011) have recently proposed the Salerno Creek deformation zone (SCDZ), a high strain mylonite zone. This structure had initially been suggested as a contractional feature (Easton and Kamo 2011), though Barshi (2012) has more recently found consistently conflicting and extensional shear sense. The outcrop which I have sampled and studied is an expression of the SCDZ and is composed of anorthositic gabbro (Figure 2). The major minerals in this rock are plagioclase and hornblende, with plagioclase being generally more abundant. This outcrop occurs on route 507 near Gooderham, Ontario and is directly south of the Glamorgan gabbro and northwest of the Anstruther gneiss complex. The location is very near to the boundary between the Harvey-Cardiff domain (to the east) and the Bancroft terrain (to the west). The rocks in this outcrop are variably strained over a relatively small space (about 25 meters). There are several centimeter to meter-scale shear zones throughout the outcrop with apparently high strain rocks, interspersed with rocks that show relatively little strain and a relict igneous texture.

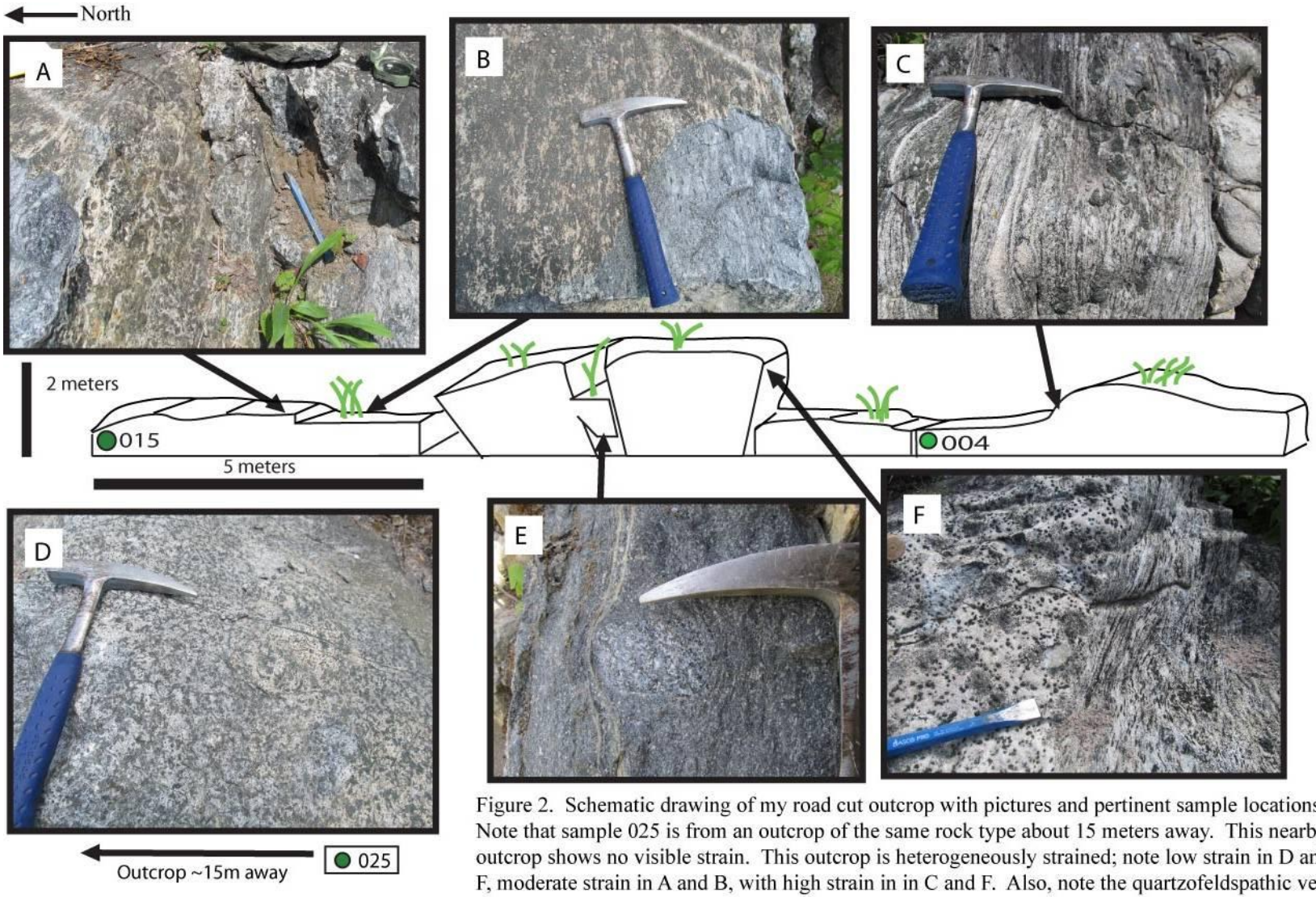

Figure 2. Schematic drawing of my road cut outcrop with pictures and pertinent sample locations. Note that sample 025 is from an outcrop of the same rock type about 15 meters away. This nearby outcrop shows no visible strain. This outcrop is heterogeneously strained; note low strain in D and F, moderate strain in A and B, with high strain in in C and F. Also, note the quartzofeldspathic vein or dike in the right of C.

2. Strain Localization and Rock Weakening

There are a variety of mechanisms which can weaken rocks and initiate strain localization. These have been well documented and interpreted over the past few decades (White et al. 1980, Kirby 1985, Bercovici and Karato 2003). Weakening mechanisms include stress concentration, reaction softening, shear heating, thermal perturbation, textural changes, introduction of fluids and formation of melt. In each of these cases there is a change in some characteristic of the rock that affects strength. These characteristic changes are observable and measurable in rocks; one can say that each leaves a distinctive fingerprint that is discernible in the rock. A complicating factor is that various weakening mechanisms can act simultaneously with one another dynamically affecting rock strength. Additionally, progressive deformation can wipe out evidence of previous textural characteristics.

By documenting the differences between low and high strain rocks, I hope to discern the weakening mechanism fingerprint and make some suggestion on what induced strain localization in the rocks I am studying. This will not be a process of simply searching for an exact 'cookie-cutter' fingerprint in the rocks of various weakening mechanisms. Instead, I will be examining changes in the rock across the strain gradient that may fit into the framework of what is known about how rocks can be weakened. Here, I will detail mechanisms of strain localization and what changes take place in rocks as they act.

A change in the minerals that constitute a rock can result in change of the bulk strength of that rock (White et al. 1980). For example an alteration of feldspar to mica

(the latter of which is a weaker mineral) can result in overall weakening of the rock if such changes are pervasive. An introduction of weak minerals can result from metamorphic and metasomatic processes (Wintsch et al. 1995). In this case we might look for the presence of weaker minerals in more highly strained rock, like phyllosilicates or calcite which would make the rock weaker. Conversely we might look for the removal of stronger minerals in high strain rock (Davis and Reynolds, 1996).

Even if there is not a change in the minerals that constitute a rock these processes can chemically change minerals to make them weaker. These can include the introduction of water into the crystal structure of a mineral. This would fall under the category of fluid related weakening which can also include the introduction of fluids along grain boundaries, leading to more mechanical weakening (Kronenberg et al. 1990). Indicators of this weakening mechanism include the presence of hydrous minerals, increased water content and pathways for fluids to move through such as fractures and veins.

Weakening can also be a result of textural changes to a rock. Grain size reduction is one such mechanism which can cause a switch a faster dominant creep mechanism. Similarly, in some creep mechanisms strain rate is dependent on grain size. This is thought to be exemplified in mylonite zones where progressive grain size reduction apparently leads to progressively weaker rheology and greater deformation (Rybacki and Dresen 2004). In addition to grain size, grain shape and orientation can also be related to weakening. If grains are anisotropic in terms of strength, the rotation of grains into the plane of shear can lead to weakening (Davis and Reynolds, 1996). Shape and crystallographic preferred orientation can be useful in determining whether grains have

been reoriented in a rock. Similarly, if a weaker mineral becomes interconnected, it can lead to a bulk weakening of the rock by allowing strain to partition in the phase that is weaker (Handy 1994, Holyoke and Tullis 2006). In both of these cases we would look for interconnection and alignment of minerals as indicators that this weakening mechanism is acting.

Thermal perturbations, the addition or subtraction of heat, can also have significant effects on rock strength. A warmer rock will generally be weaker than a cooler rock, so magma intrusion, introduction of hot fluids and advection of hot material can all weaken rocks and localize strain. Nearby dikes or magma intrusions would point to the influence of thermal perturbations. Also, formation of melt in a hot rock can lubricate grain boundaries and produce weakening and we would look for evidence of this in thin section (Misra et al 2009). Deformation and shearing of a viscous material leads to the release of energy in the form of heat which can further weaken rocks, though the potential for this mechanism to localize deformation is debatable (Crameri and Kaus 2010).

In some cases stress can be concentrated instead of uniform when some strength heterogeneity redistributes stress in the rock or the shape of the body under stress causes stress to be transferred (Montesi and Zuber 2002). Under higher stress, rock deform at a higher strain rate, so strain localization can be initiated. By stress concentration, strain can localize at strength contrast boundaries such as lithologic contacts and cross-cutting dikes. With these mechanisms of weakening and localization in mind, I will examine my rocks of interest and compare what I observe with what is known about rock deformation.

METHODS

1. Field Methods and Sampling

In order to investigate the relationship between strain and microstructural characteristics in this outcrop, I collected samples that were representative of the widely varying degrees of strain within the outcrop. My general goal was to select samples that fit into the categories of high strain, moderate strain or low strain, with attention to covering the spatial extent of the outcrop (Figure 2). To these ends, I collected 16 oriented and labeled samples. Four of these samples appeared highly strained, 5 appeared moderately strained and 7 exhibited low to no visible strain. Of these samples, 2 contain round nodules of apparently undeformed rock surrounded by moderately strained rock. Four of the low to no strain samples are from an outcrop that is not continuous with the main outcrop but is similar in rock type and is 15-25 meters north. From these samples I selected 3 for more detailed work, one from each of the low, moderate and high strain categories.

2. Thin Section Preparation

For the purpose of microanalysis, I prepared thin sections from these three hand samples. These samples were selected on the basis of ease of thin section preparation and their representation of desired features, i.e. low, moderate or high degree of strain. The thin sections that were polished for microanalysis were cut parallel to lineation and

perpendicular to foliation. In the highly strained samples, lineation and foliation were visibly apparent, but this was not the case for moderately strained and highly strained samples. In order to cut samples in the desired orientation I calculated the regional average orientations of both lineation and foliation and applied this to my rock cutting. Samples were carbon coated and chemically polished with colloidal silica as necessary for analysis.

3. Microanalysis

The samples I selected for microanalysis were numbered 004 (high strain), 015 (moderate strain) and 025 (low strain). Two thin sections were taken from each of the two latter samples and six were taken from 004 (only two were used for analysis). To estimate modal mineral percentages I used image processing software, applying a color threshold to determine the percent of light and dark minerals. To analyze mineral chemistry of hornblende and plagioclase I used wavelength-dispersive X-ray spectroscopy (WDS). This was conducted using the University of Maine's Cameca SX100 Electron Microprobe (EMP). For the purpose of gathering grain data, including crystallographic preferred orientation (CPO), shape preferred orientation (SPO), grain aspect ratio and grain size, I used electron back-scatter diffraction (EBSD) (Figure 3). These analyses were performed using the University of Maine's Vega II XMU Scanning Electron Microscope (SEM) and TSL-OIM Data Collection and Analysis software. Additionally, I used the SEM for creating backscatter electron (BSE) maps of my thin sections.

WDS

When the EMP accelerates electrons at a sample, an incident electron may excite an electron of the inner shells of an atom causing the atom to eject that electron. To replace it an electron from a higher energy shell moves to a lower energy state giving off an x-ray in the process. The wavelength of this x-ray is characteristic of the shells which the electron has moved between and thus characteristic of the type of atom which it has emitted from. So, by measuring the number of x-rays of specific wavelengths which are emitted we can quantify the abundance of different types of atoms, that is, the chemical composition of a material of interest. For this analysis the beam was focused to 5μm, with an accelerating voltage of 15kV, 10nA current and 0.267 second count time. For one thin section from each strain level I collected 20-50 measurements of the chemical composition of plagioclase and hornblende, with attention to differences in texture and grain size for sampling.

BSE

Electrons that are fired at a sample using the SEM are scattered back from the sample after interacting with the material's atoms. Atoms with greater mass backscatter electrons more strongly and so by measuring the strength with which electron are backscattered from specific locations one can measure, in a relative sense, how heavy the atoms in that material are and the general composition of that material. Heaviness of the scattering material is analogous to brightness on a BSE image. My samples are

composed primarily of hornblende and plagioclase. Hornblende is much richer in heavier elements like iron and magnesium than plagioclase, so it appears much brighter on a BSE image. This is useful for an overall picture of the rock mineralogy and structure. BSE maps were taken for each thin section that I studied (Figure 4).

Mineral Modes

The samples of this study are composed primarily of hornblende and plagioclase; in most thin sections they constitute more than 95% of the section. On BSE images these minerals appear light (hornblende) and dark (plagioclase) which makes it possible to use a grayscale threshold value to approximate the modal percent of each mineral in a sample. Using image processing software, I measured approximate modal mineral compositions with threshold values between 140 and 214. I performed this procedure for all of my thin sections.

EBSD

Electron back-scatter diffraction is an SEM technique used to measure the orientation of a crystalline material (Figure 3). When an electron beam is focused on a sample at a low angle, the electrons interact with the crystalline structure and diffract off the sample, forming a specific pattern related to the crystal structure, when they hit a phosphorous screen detector. These diffraction patterns are photographed on the detector screen. The pattern of electrons hitting the screen will be different depending on the

orientation and type of crystalline material that is being analyzed and can thus be used to infer the orientation of a mineral in thin section. However before the orientation of a mineral can be determined we must find out what mineral it is. Similar to the WDS process, EBSD uses energy dispersive x-ray spectroscopy (EDS), to measure chemistry and determine the minerals present using emitted x-rays.

With mineral identity, the diffraction pattern can be matched to a specific crystalline structure and specific orientation of that crystalline structure. EDS data and diffraction patterns were collected using a scanning electron microscope. The electron beam was set to scan across a designated area of the sample, dwelling briefly at tiny preset intervals to collect a diffraction pattern and x-ray data. In post processing, we define the minerals present and their locations in the area and the diffraction patterns are matched to a specific orientation at those locations. This gives us the mineral identity and its orientation at every location in an analyzed area.

For this analysis I used a step size between 8 and 12μm, 70˚ sample tilt, ~25mm working distance, accelerating voltage of 20kV and a probe current of 10nA. The result is a map of the scanned area showing mineral type and crystallographic orientation. I performed EBSD analysis on 2-3 areas on each thin section. From this, the data were processed using TSL-OIM programs to distinguish mineral grains on the basis of composition and common crystallographic orientation of the measured points. Grains were defined as having 2 or more pixels and more than 5˚ misorientation from neighboring pixels. I used TSL-OIM Analysis to refine and clean up the data with neighbor orientation correlation and grain size dilation routines. This same program was used to make calculations of grain size, CPO, SPO and grain aspect ratios. For further

collation and organization of SPO, grain aspect ratio and grain size data I used Microsoft Excel to produce the graphs that you see in this volume.

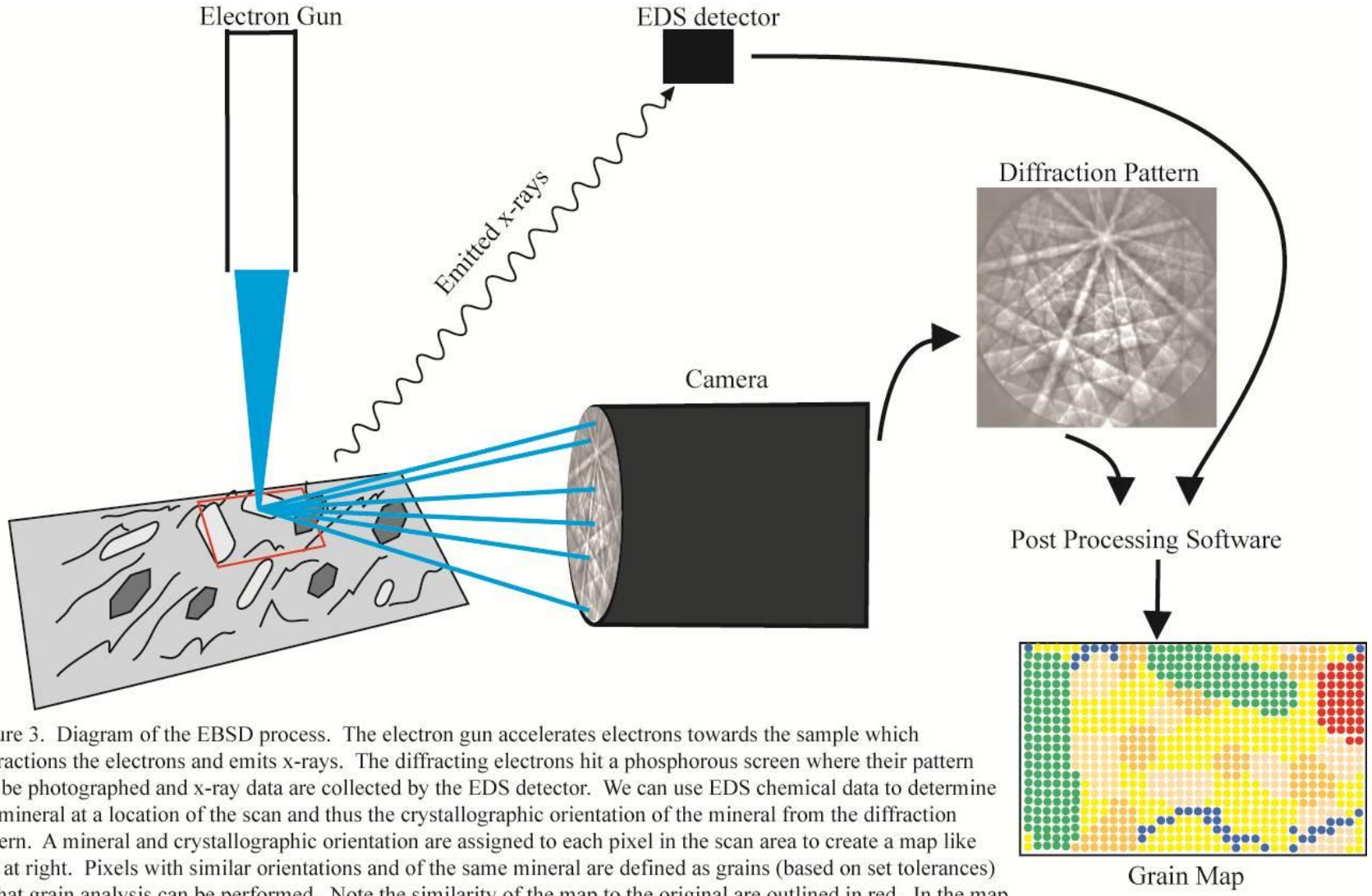

Figure 3. Diagram of the EBSD process. The electron gun accelerates electrons towards the sample which diffractions the electrons and emits x-rays. The diffracting electrons hit a phosphorous screen where their pattern can be photographed and x-ray data are collected by the EDS detector. We can use EDS chemical data to determine the mineral at a location of the scan and thus the crystallographic orientation of the mineral from the diffraction pattern. A mineral and crystallographic orientation are assigned to each pixel in the scan area to create a map like that at right. Pixels with similar orientations and of the same mineral are defined as grains (based on set tolerances) so that grain analysis can be performed. Note the similarity of the map to the original are outlined in red. In the map distinct grains are mapped as having different colors.

RESULTS

1. Assumptions

At the outset of this research there are a few things that should be taken into consideration. Weakness in these rocks will result either from inherent weaknesses of the unstrained parent or from weaknesses induced by some process. Ideally, to discover the sources of rock weakness we would be comparing rocks from a single shear zone and a single strain gradient so that there would not be the uncertainty of whether or not these rocks were different to begin with. This is not the case; the samples which I have compared are from different parts of the outcrop and not from the same shear zone. Though this is not an ideal situation there do not seem to be extreme differences in the rock across the outcrop apart from strain, so the comparisons I have made can still be meaningful.

2. Samples

004by and 004ey

004by is a high strain sample with foliation running perpendicular to the long direction of the thin section slide (Figure 4). There is distinct segregation of hornblende and plagioclase but there is plagioclase in the hornblende domains and vice versa. There is no biotite in 004by but there is occasional titanite. There is chlorite and sericite

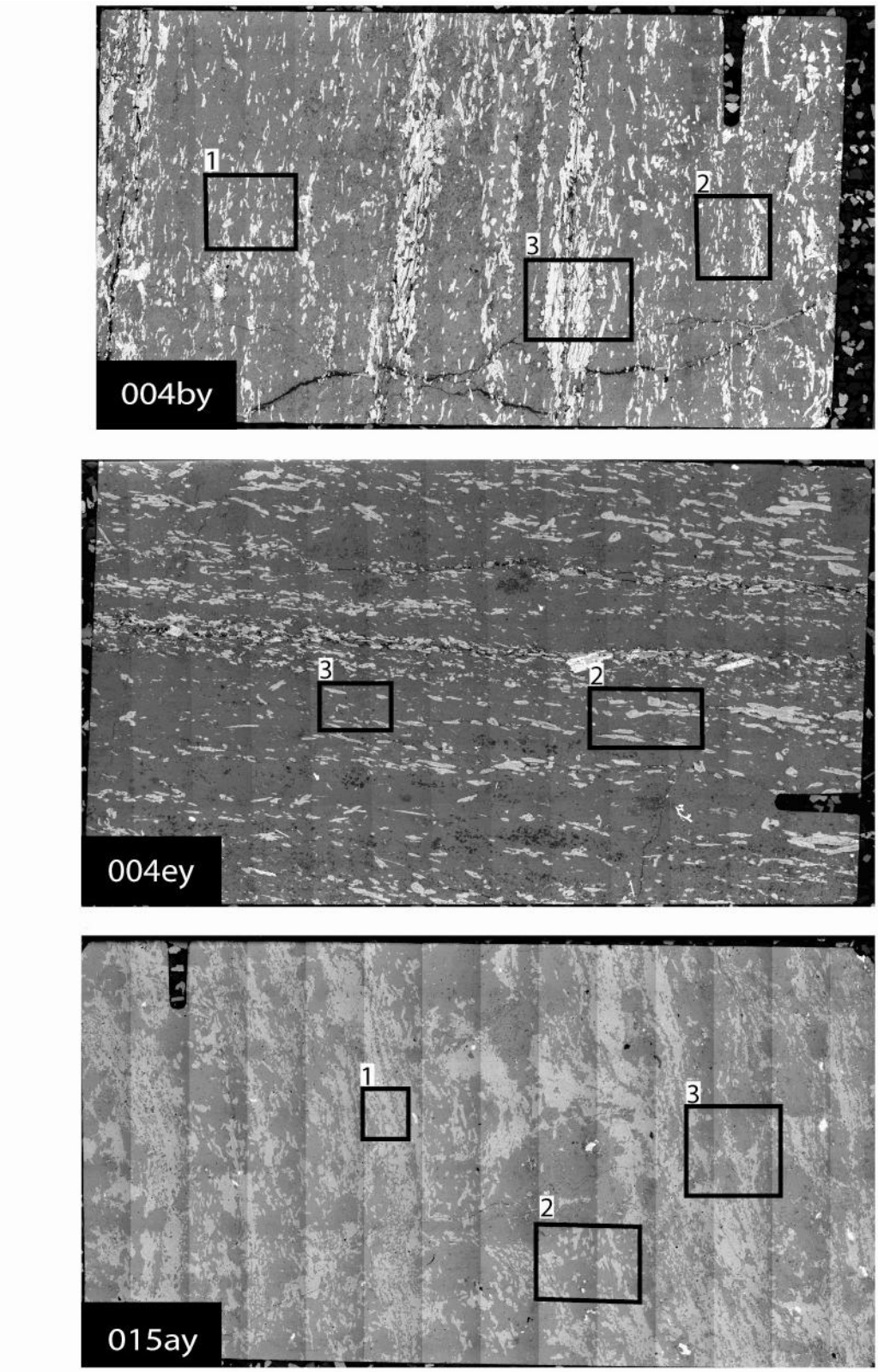

Figure 4. Backscatter electron images of each thin section analyzed. EBSD areas are outlined in black and numbered as appears in all off the following data graphics. Plagioclase is always the dark mineral and hornblende the light. Color differences are mostly due to SEM settings.

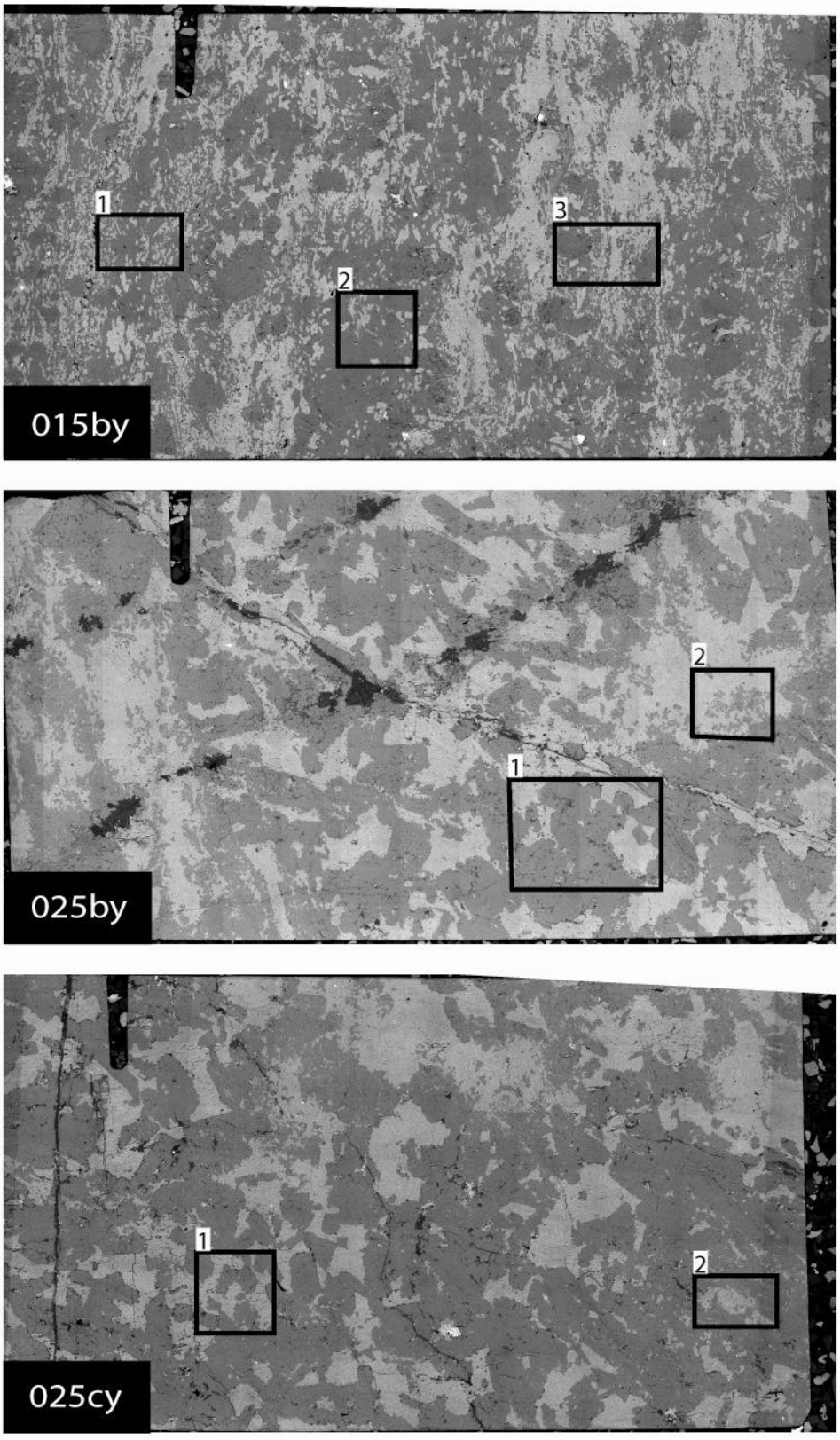

Figure 4 continued. Backscatter electron images.

alteration present. I selected three areas on which I performed EBSD analysis. One area was over a hornblende domain (3) and the other two were in the plagioclase rich domains (1, 2) (Figure 5). In each of the latter, the grain size and texture of hornblende seems slightly different so I sampled both to be representative of the whole thin section.

Sample 004ey is a high strain section from the same rock sample as 004by (Figure 4). In this section foliation runs parallel to the long direction of the thin section. Hornblende and plagioclase rich domains are less distinct but are present. Biotite composes up to 5% of this sample and minor titanite is present. Two areas were analyzed using EBSD representing slightly different hornblende grain sizes (Figure 6).

015ay and 015by

Sample 015ay is a moderately strained sample (Figures 4). Foliation is not distinct in this rock but anastomosing bands of hornblende seem to wrap around larger plagioclase crystals. Biotite is present and comprises less than 5% of the section. I used three areas for EBSD, one covering larger plagioclase grains (3), another covering larger hornblende grains (2) and one covering a distinctly hornblende rich area (1) (Figure 7). 015by is from the same rock and is a very similar sample to 015ay the major difference being that there is very little biotite in 015by. I selected EBSD areas for both of these sections in a similar way (Figure 8).

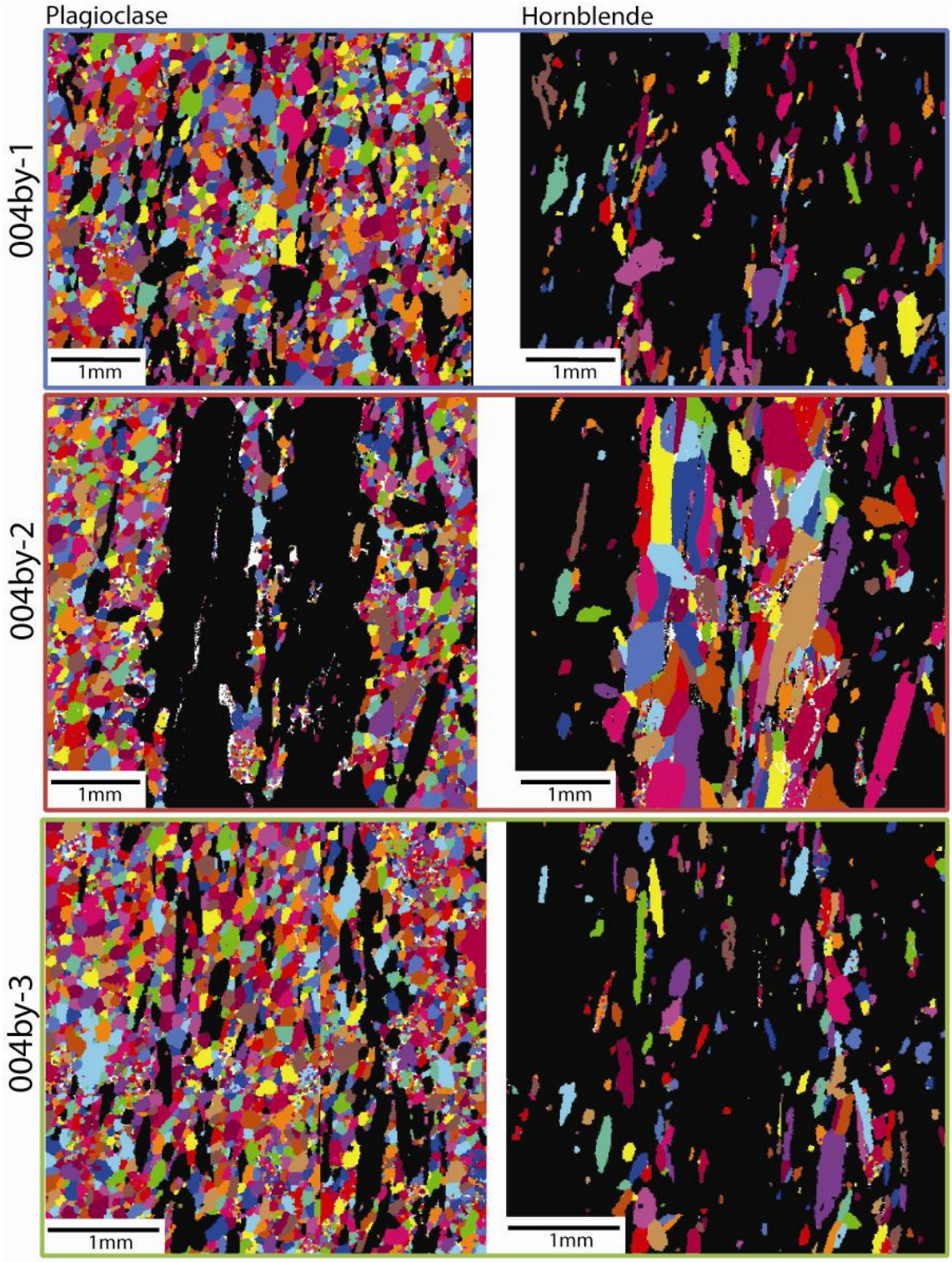

Figure 5. Unique grain maps for each of the EBSD areas that I analyzed for plagioclase and hornblende seperately. This gives an idea of the general texture of each area for the important minerals. Numbering corresponds to the numbers associated with the areas in figures 4-1 and 4-2. These are calculated using TSL OIM Analysis software. Color borders correspond to the same sample with in each degree of strain through out all of the remaining figures.

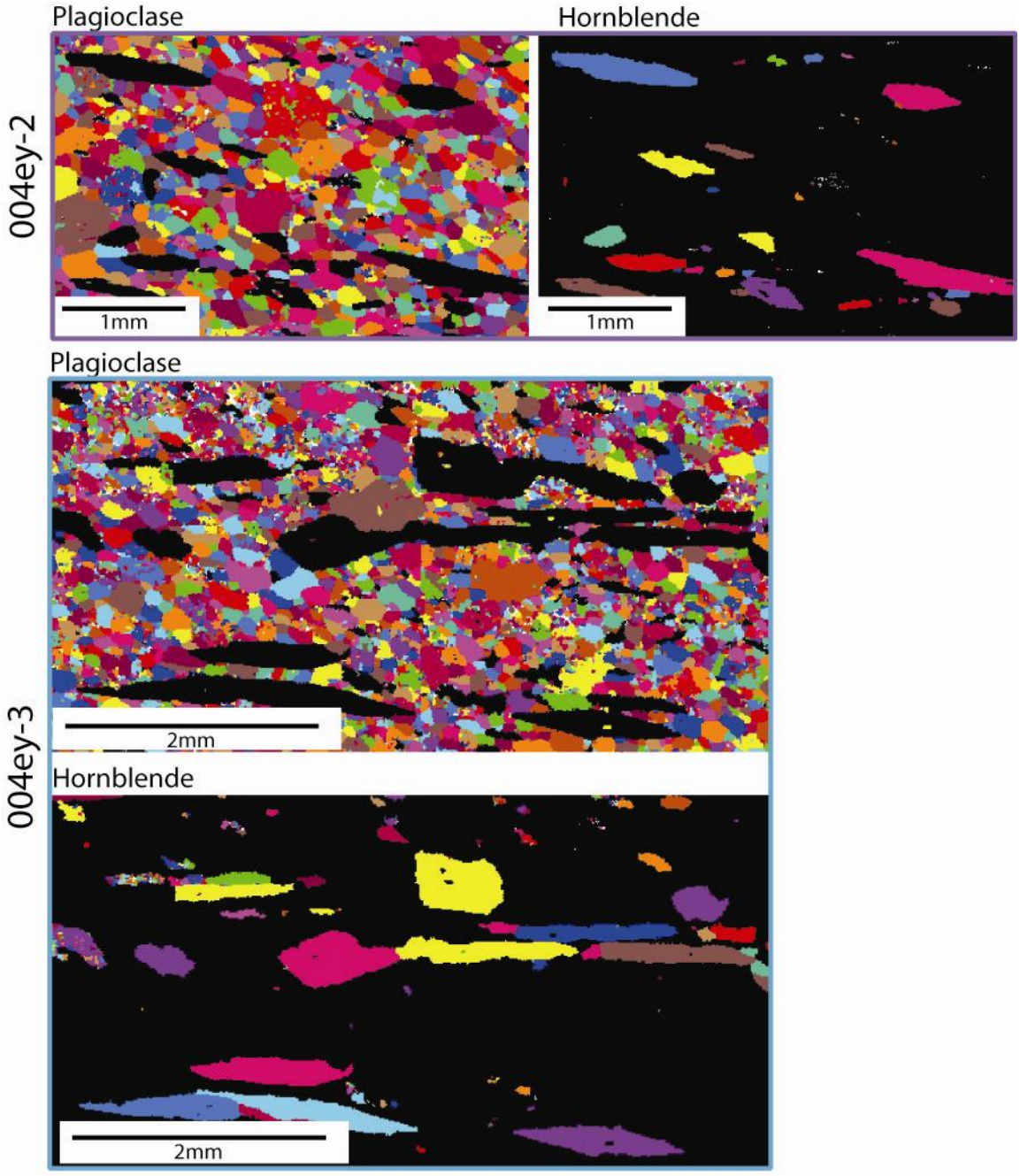

Figure 6. Additional unique grain maps for both plagioclase and hornblende.

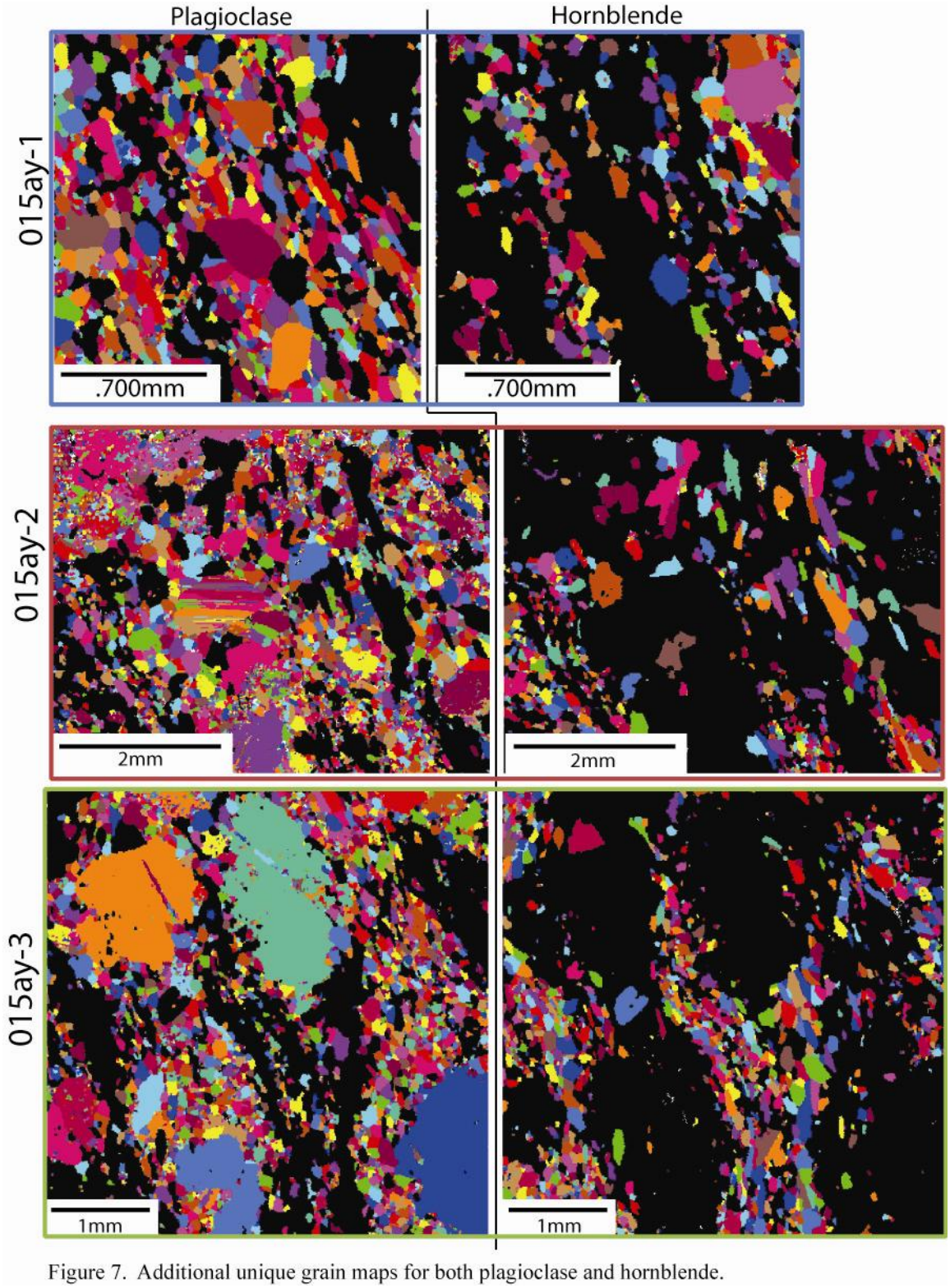

Figure 7. Additional unique grain maps for both plagioclase and hornblende.

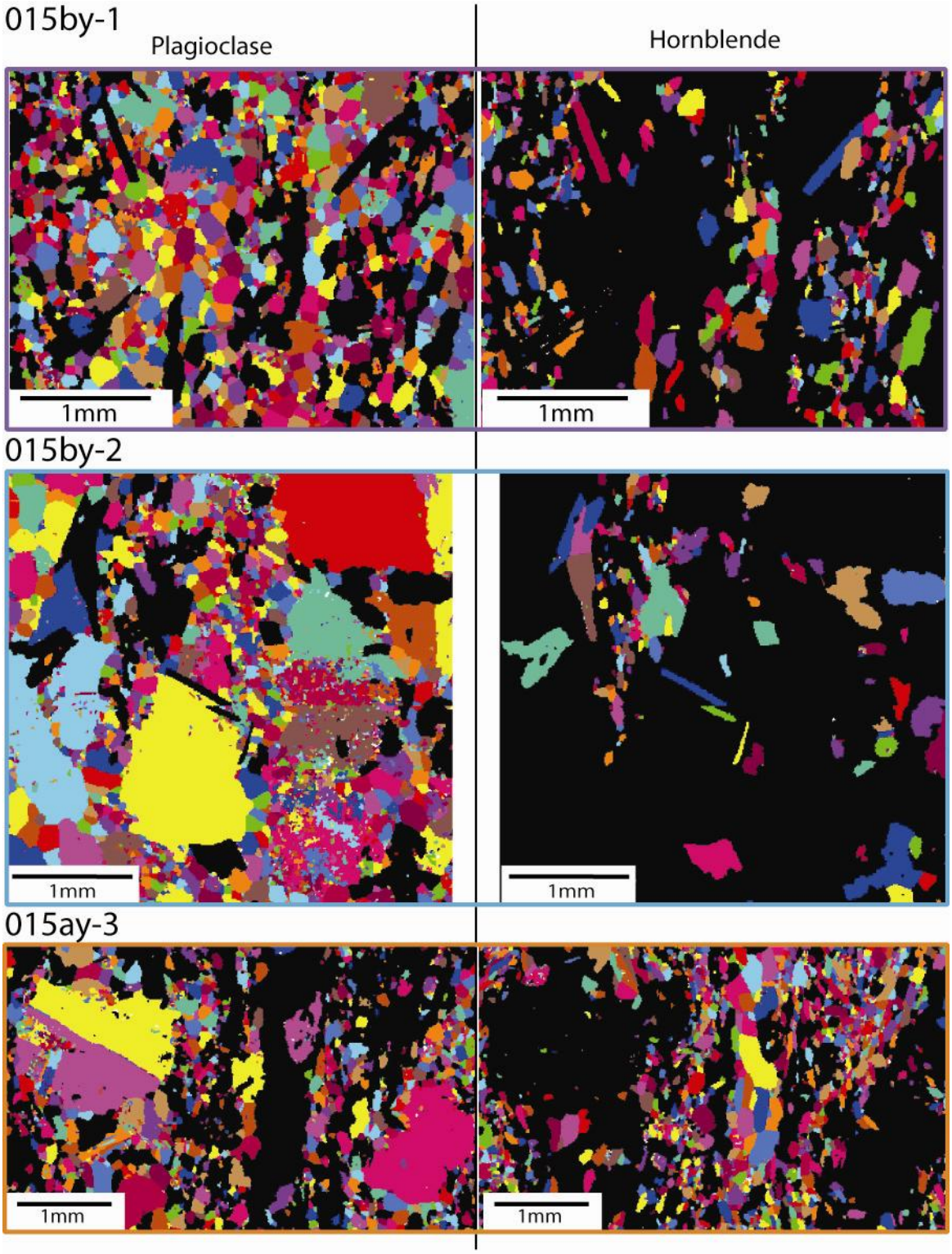

Figure 8. Additional unique grain maps for both plagioclase and hornblende.

025by and 025cy

Both of these are low strain samples exhibiting an igneous texture (Figure 4). Plagioclase grains are relatively euhedral and randomly oriented. No biotite is present in either sample; there is minor tourmaline in 025by. I selected two areas on each of these sections for EBSD analysis (Figure 9 and 10). One area on each exhibited igneous texture (1) while the other covered a small recrystallized patch.

3. Textures

On the hand sample scale, low strain samples exhibit igneous textures with no foliation or lineation (Figure 11-1A). High strain samples show smaller grain sizes and strong gneissic foliation defined by compositional banding of alternating hornblende-rich and plagioclase-rich layers (Figure 11-1B). Noteworthy at the mesoscale, is the presence of several small quartzofeldspathic veins in the outcrop that are often within highly strained areas (Figure 2C). At the optical microscope scale, the major difference between high and low strain rocks is the proportion of recrystallized and grain size reduced plagioclase and hornblende in the sample (Figures 11-1A and 11-1B). The low strain rocks have mostly large grains with abundant deformation and albite twinning and little recrystallization or grains size reduction (Figure 11-1A). Occasionally plagioclase twins are bent. Low strain samples exhibit minimal plagioclase recrystallization in small, disconnected patches (Figure 11-1C).

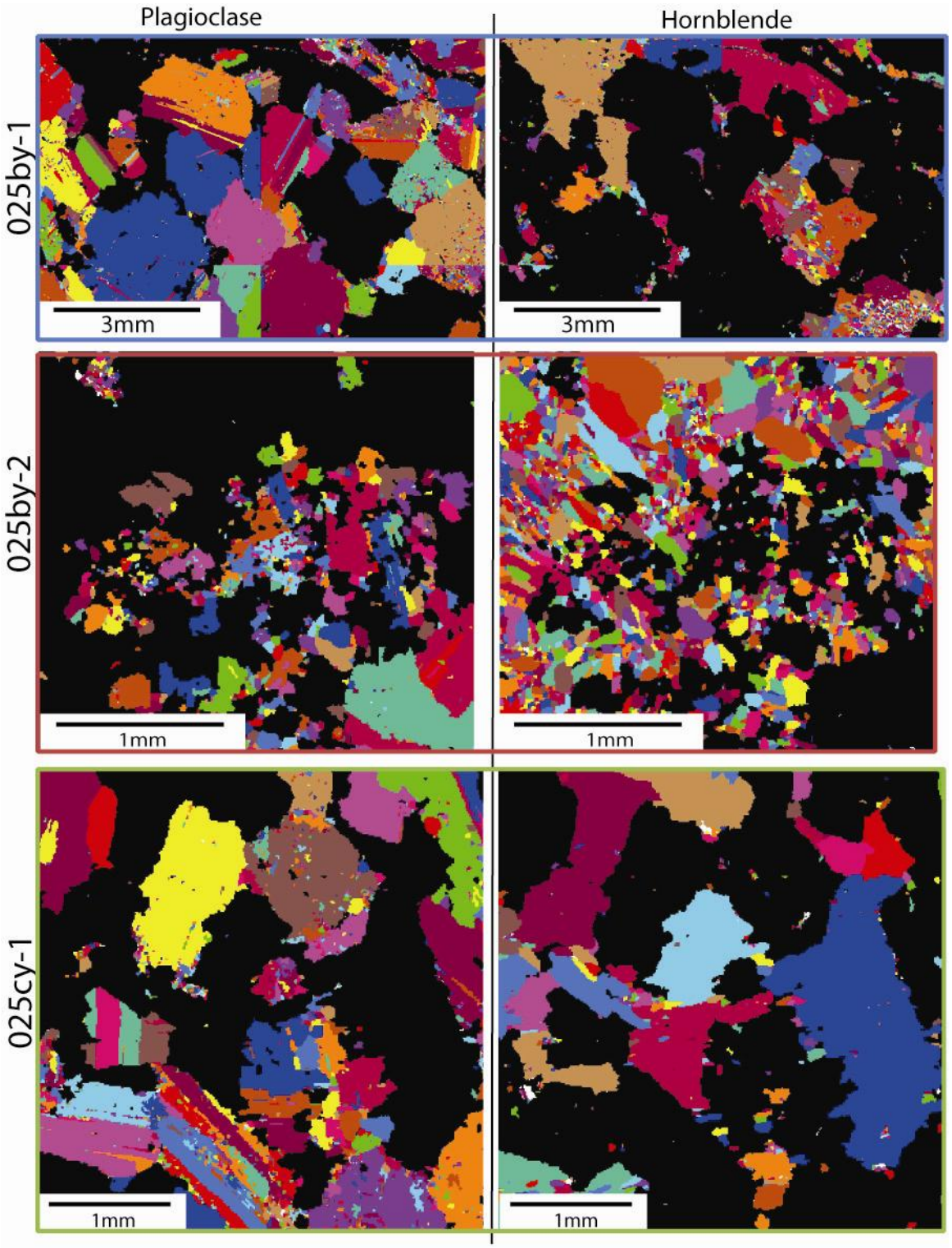

Figure 9. Additional unique grain maps for both plagioclase and hornblende.

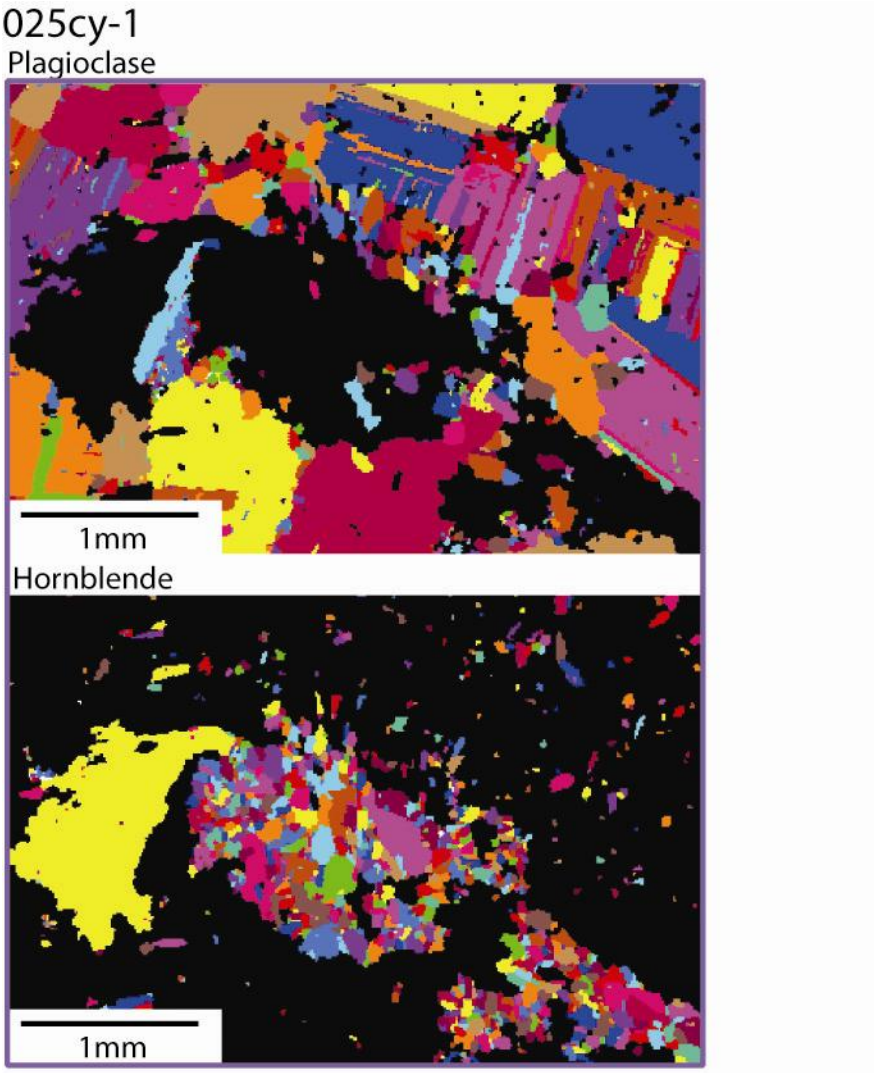

Figure 10. Additional unique grain maps for both plagioclase and hornblende.

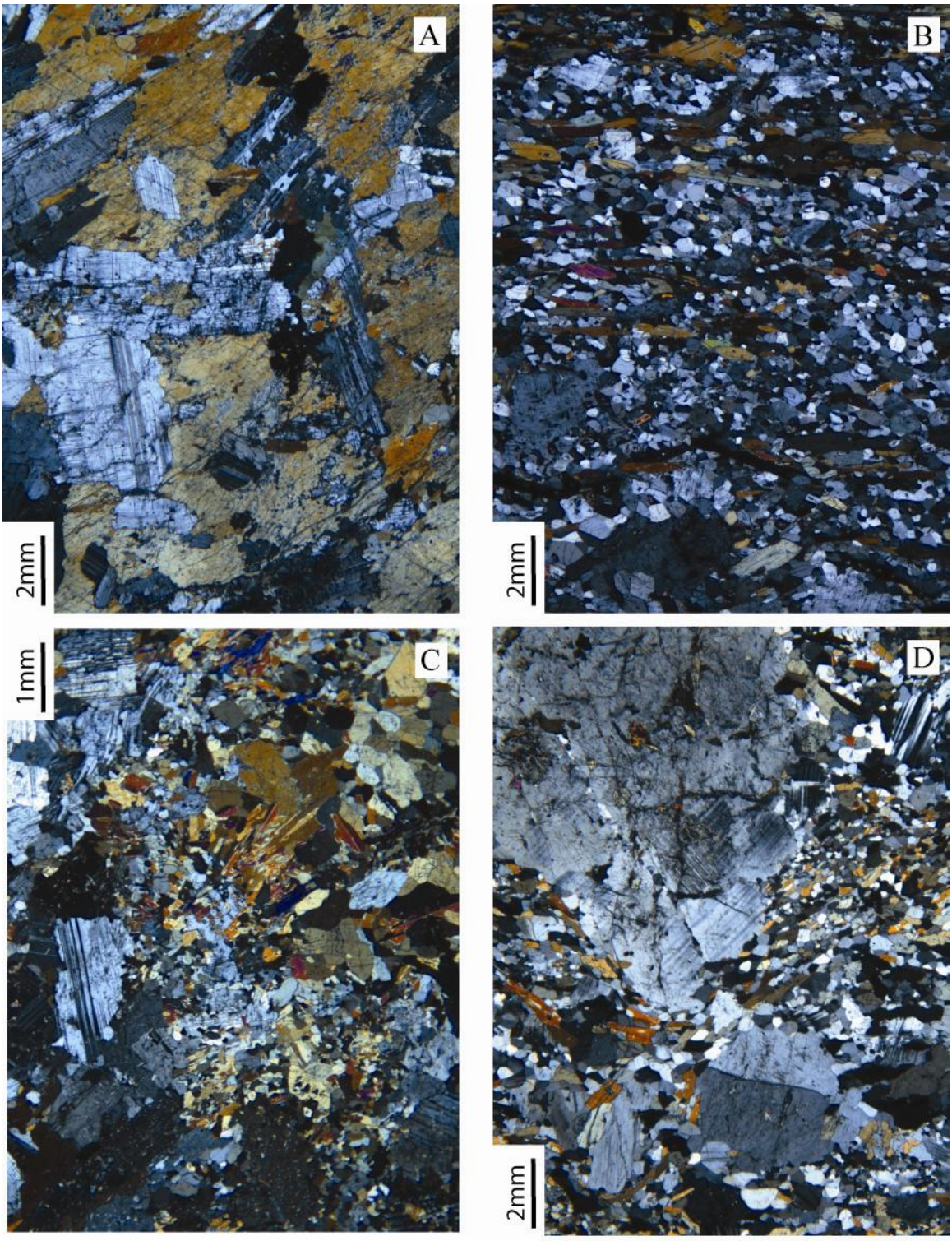

Figure 11-1. Photomicrographs of thin sections in cross polarized light. A) shows the igneous texture of the low strain samples and B) shows that prevasively recrystallized high strain samples with rare large plagioclase grains and aligned hornblende grains. C) shows a small recrystallized patch with the high strain rocks. D) shows the general texture of moderate strain samples with more abundant large plagioclase grains and also subgrains forming along the fracture in the large plagioclase. See text for more details.

The high strain samples contain plagioclase that is fine grained and almost completely recrystallized throughout the thin section. Large plagioclase grains are rare but present in the high strain rocks (Figure 11-1B). In some locations the plagioclase has a core and mantle texture with small grains within and around the large grains, often in distinct lines that may mark intergranular fractures (Figure 11-1D). The moderately strained samples are a combination of the two end-member strain types, having large grains as well as recrystallized plagioclase and dismembered hornblende (Figure 11-2A).

In the recrystallized zones, hornblende generally has the appearance of being crushed and smeared out (Figure 11-3A). Even in the low strain samples some hornblende grains appear broken but with little displacement. In high strain samples hornblende is finer grained and disseminated throughout the matrix. Hornblende grains are interconnected in some high and moderate strain samples, but in other high strain samples they are not. There does not seem to be any correlation between hornblende interconnectedness and strain.

At all strain levels, smaller recrystallized plagioclase grains are generally free of twins and have very clean grain interiors, which is in sharp contrast to the large grains. Plagioclase commonly exhibits undulous extinct in both small and large grains. In the case of the fine grained plagioclase and the hornblende, grains often meet at triple junctions with 120˚ between boundaries (11-3B). This is not always true and especially not when there are many fine grained plagioclase and hornblende crystals close together. In this latter case, crystals that are finer grained do not as commonly have 120˚ triple junctions (11-3B).

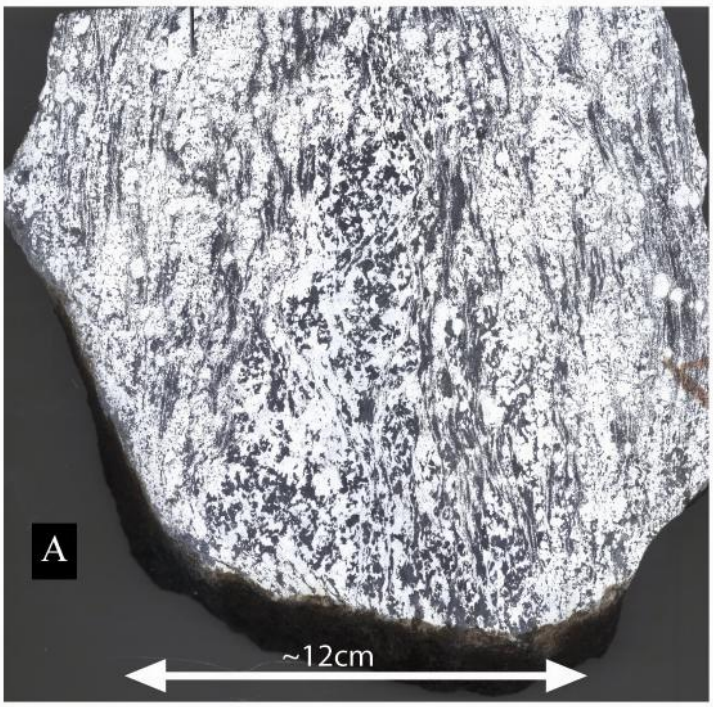

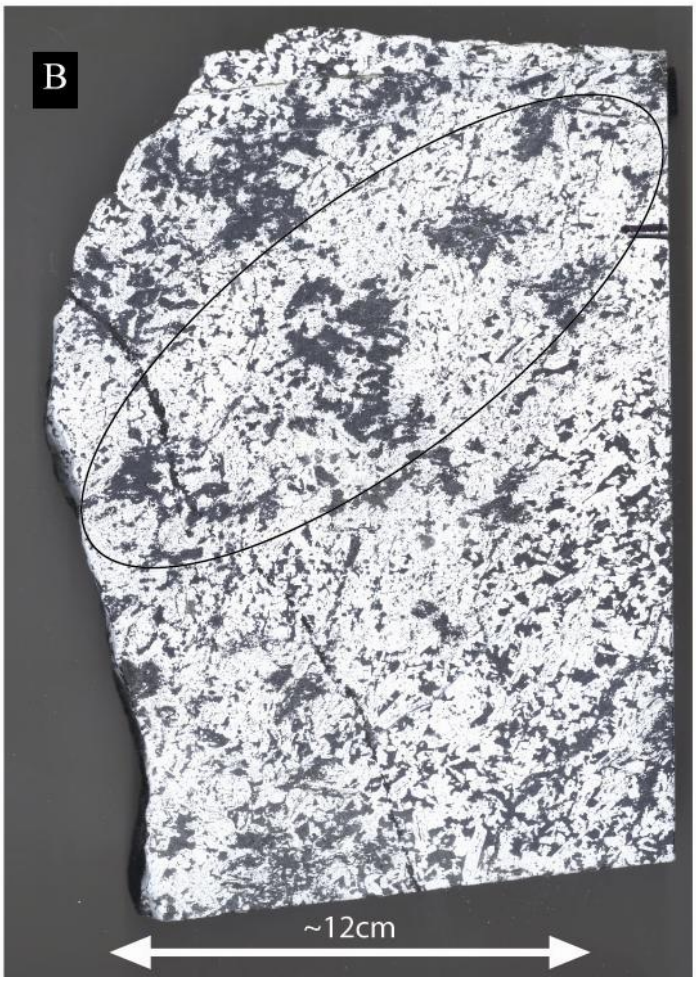

Figure 11-2. Scanned photograph of slabs of sample 015y (A) and 025y (B). They have been etched with hydrofluoric acid to show contrast between hornbende and plagioclase. Note that in A, the rock is comprise of small, relatively unstrained parcels with smearing plagioclase and hornblende anastomosing throughout. In B, the circled area highlights plagioclase crystals with less distinct boundaries which may indicate recrystallization. Hornblende seems less abundant in this area and more isolated where it is present.

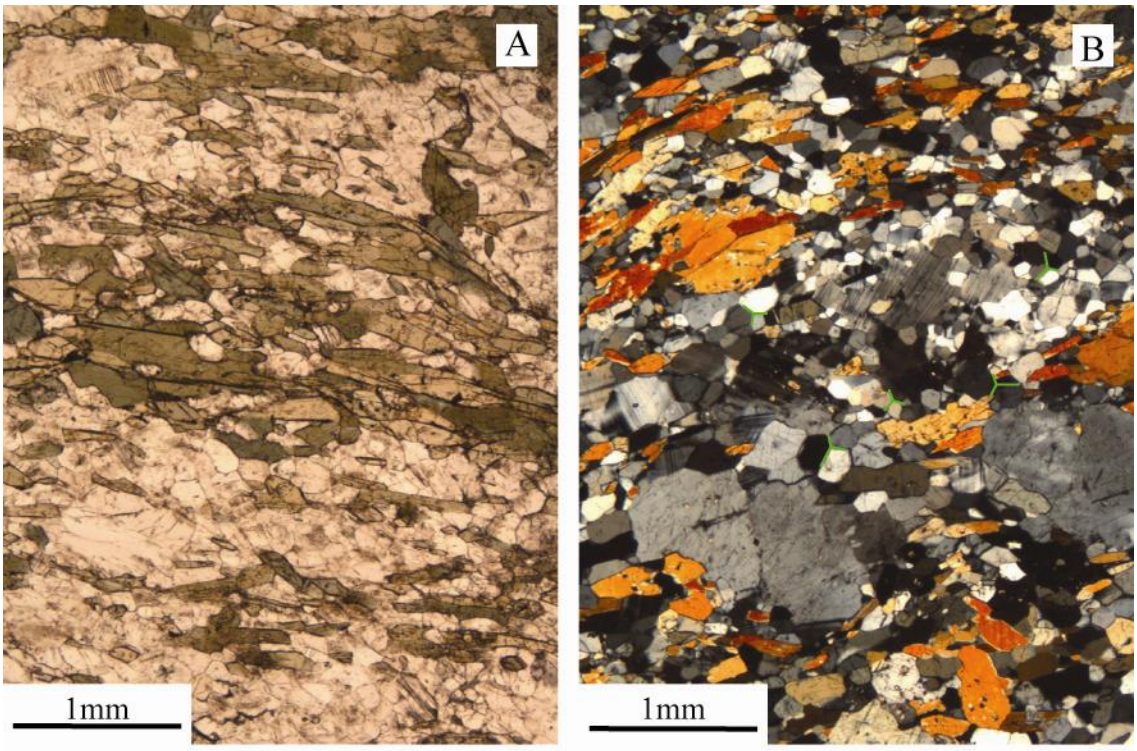

Figure 11-3. Additional photomicrographs. A is under plane-polarized light from 004cy and B is from 015ay under cross polarized light. A shows an example of hornblende brittle fracturing. B shows 120 triple junctions of plagioclase crystals, indicating recovery (few highlighted in green).

4. Grain Size

Grain size varies greatly between these samples. In the low strain samples both plagioclase (Figure 12) and hornblende (Figure 13) have large grain size, the majority of the grains being >500μm in diameter. In the moderate and high strain samples the grain sizes of plagioclase and hornblende are reduced, a large proportion of grain diameters are centered around 100-200μm for both. In the moderate strain samples, there is larger proportion of the original larger plagioclase grains than in the high strain samples. This is less true for hornblende; few large grains are present in the moderate strain samples and the distribution of grain sizes is much less regular than that of plagioclase.

In the high strain rocks, almost all of the plagioclase is small and recrystallized, though rare large plagioclase grains remain. In comparison to moderate strain samples hornblende grains are somewhat larger in the high strain samples. This distribution is somewhat overwhelmed by a great number of larger hornblende grains from areas 004ey-2 and 004ey-3. Still, the hornblende grains are larger in the high strain samples. In each of the low strain samples, the EBSD areas of small recrystallized material resemble the grains size distribution of the higher strain samples. This is more pronounced for hornblende than for plagioclase.

From low to high strain plagioclase shows a clean progressive grain size reduction. The large grain sizes give way to a mixture of small and large grain sizes in the moderate strain samples and to a consistent smaller grain size in the high strain samples. This progression is not as clean in hornblende, where grains are somewhat larger in the high strain samples, though still reduced from the low strain samples.

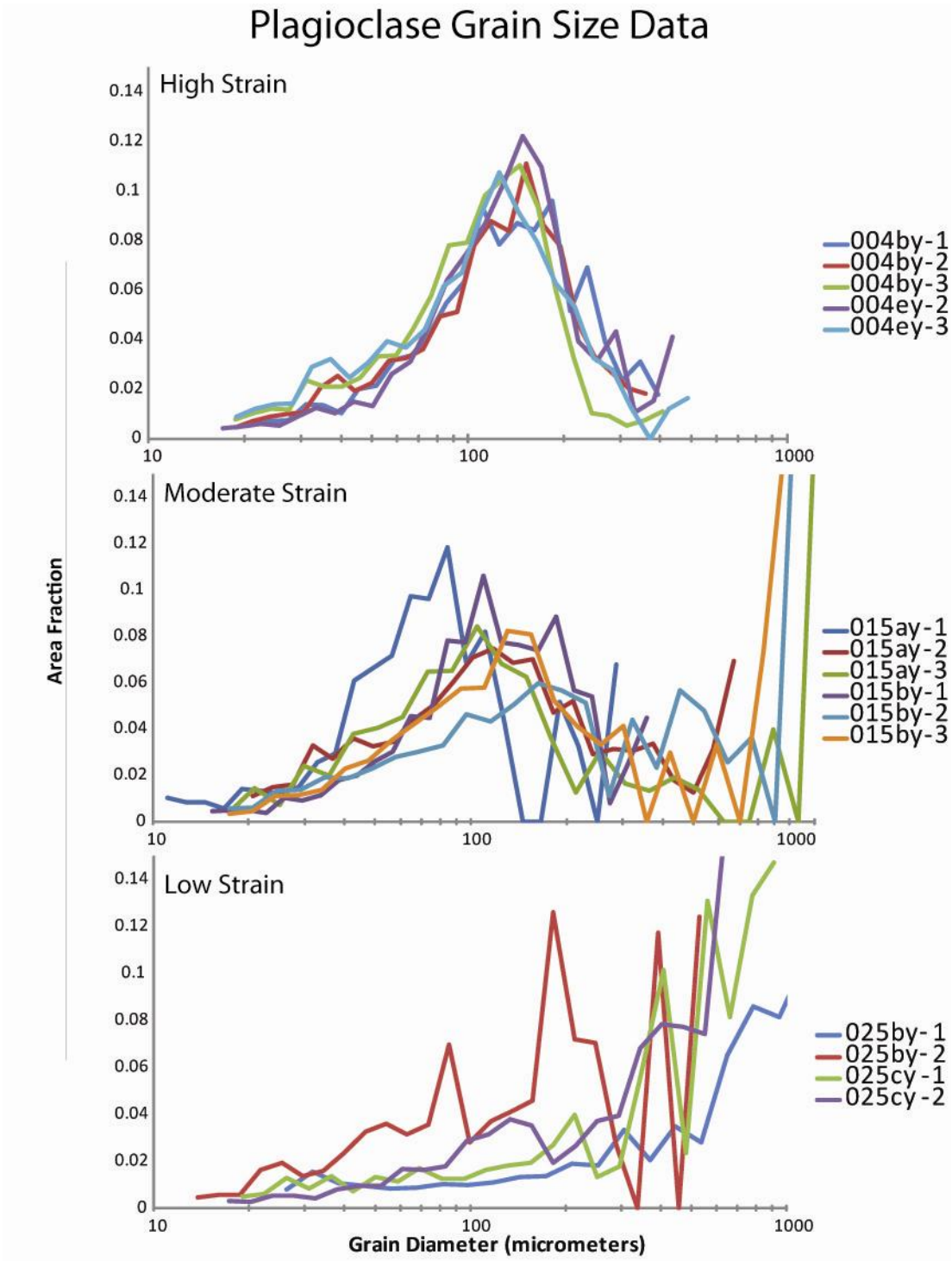

Figure 12. Results of plagioclase grain size analysis across the degrees of strain. There is a consistent grain size reduction with greater strain. See text for more details.

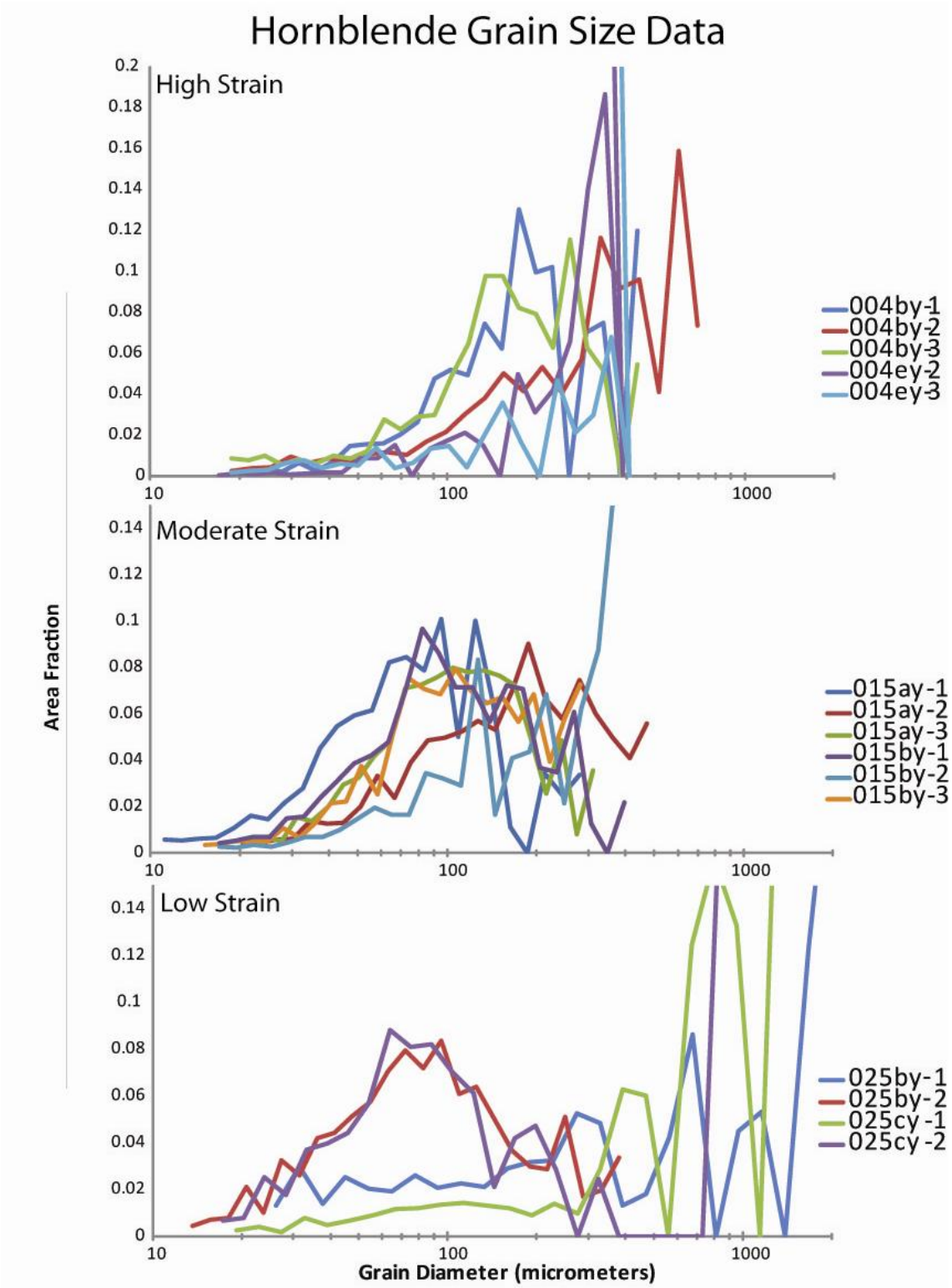

Figure 13. Results of hornblende grain size analysis across the degrees of strain. There is a grain size reduction from high to moderate strain with a slight increase in grain size in the high strain. The high strain distribution is somewhat overwhelmed by by 004ey-2 and 004ey-3 which could be misleading. See text for more details.

5. Crystallographic Orientation

In the low strain rocks there is no discernible CPO; largely because in most cases there are too few grains to define a distinct common orientation (the grains are very large in comparison to the scan areas). In low strain areas that did contain enough grains, the patterns of axis orientations are diffuse in both plagioclase and hornblende; they do not define any CPO (Figure 14 and 15).

In most moderate strain samples plagioclase does not have a CPO; in one or two areas there is an extremely weak pattern in the crystallographic axes but in most the patterns are diffuse (Figure 16). Hornblende in moderate strain shows a strong CPO which is somewhat different from that of high strain samples. C-axes are generally aligned in the plane of foliation and a-axes are preferentially aligned perpendicular to foliation in most samples though there is some variation. B-axes are not commonly aligned in moderate strain (similar to the high strain) (Figure 17).

In high strain samples c-axes of plagioclase are very weakly aligned parallel to foliation and b-axes are very weakly aligned in a plane perpendicular to foliation. In some areas, such as 004by-1 and 004by-2, the CPO is strong than others, but it is still diffuse and weak (Figure 18). A-axes consistently show no pattern while c-axes and b-axes define what CPO is present. Hornblende exhibits a strong CPO in high strain samples. C-axes are linearly aligned parallel to foliation in the high strain sample, a-axes are aligned linearly perpendicular to foliation and b-axes do not define a strong pattern (Figure 19).

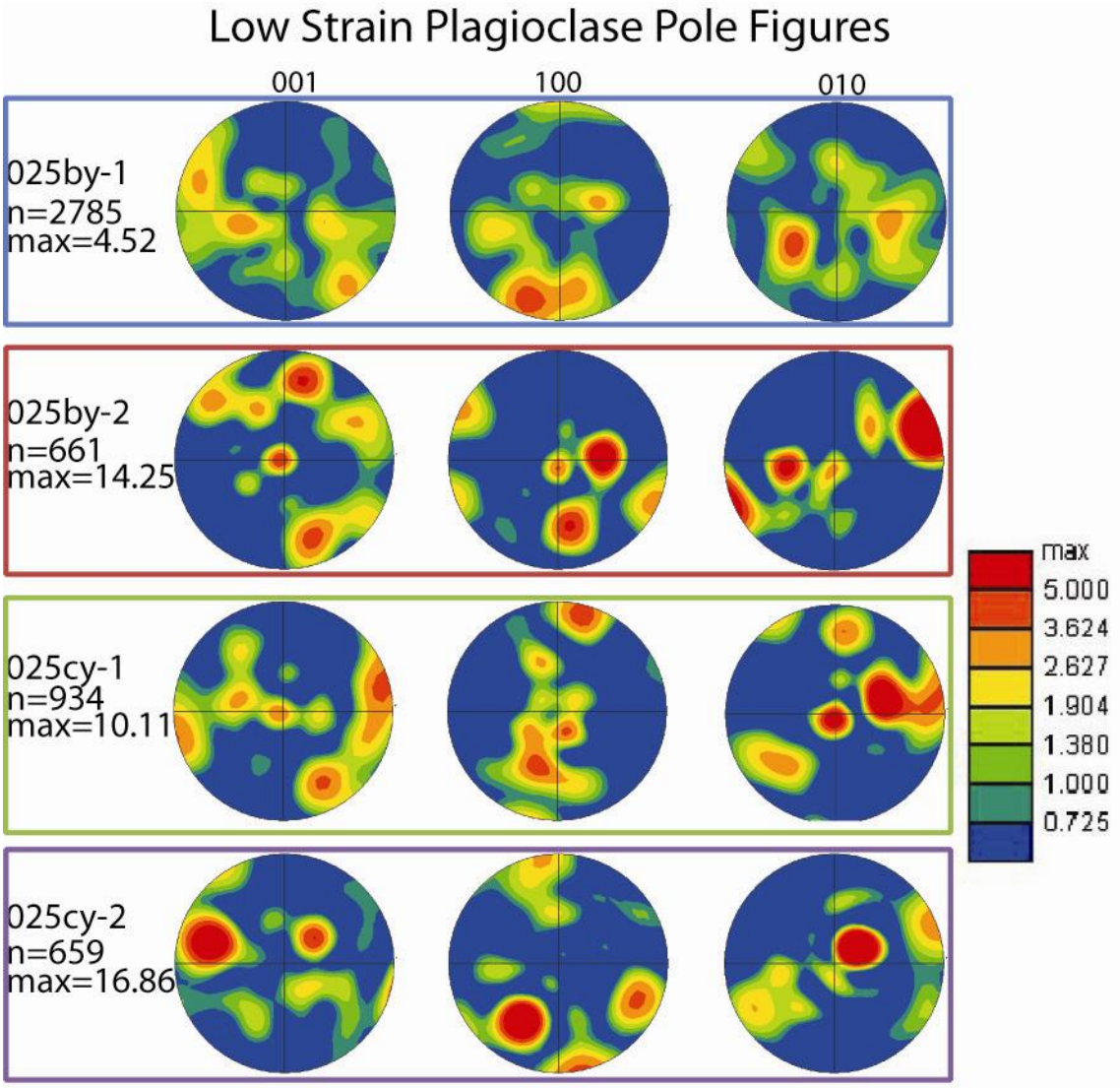

Figure 14. Low strain plagioclase pole figures of crystallographic orientation, showing minimal CPO. Note that 025by-2 and 025cy-2 are from fine grained recystallized areas. Note, 'n' is the number of grains used to construct the pole figure. 'Max' is the greatest factor by which the axes are concentrated from a uniform distribtuion and colors are scaled for this. See text for more details.

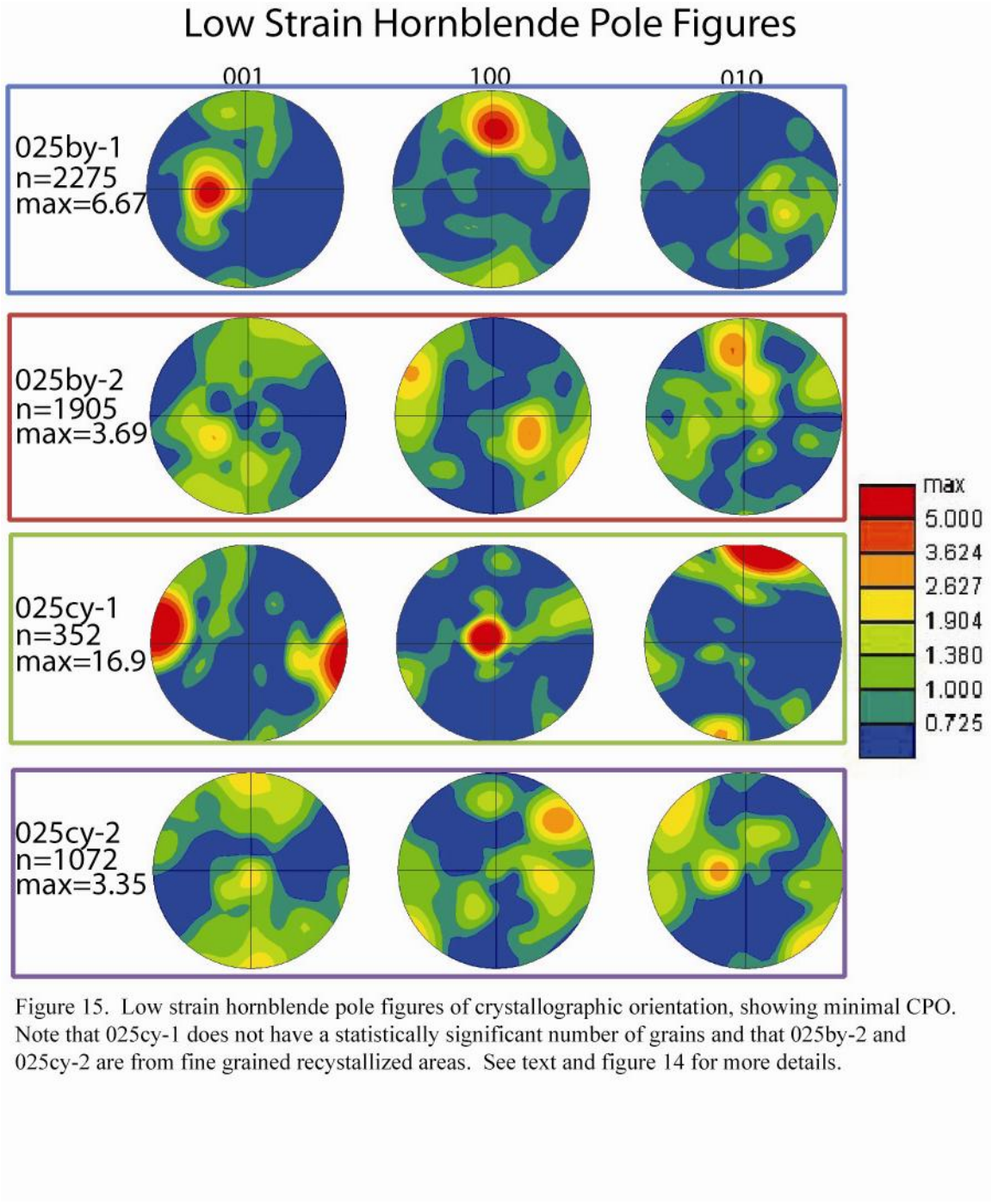

Figure 15. Low strain hornblende pole figures of crystallographic orientation, showing minimal CPO. Note that 025cy-1 does not have a statistically significant number of grains and that 025by-2 and 025cy-2 are from fine grained recystallized areas. See text and figure 14 for more details.

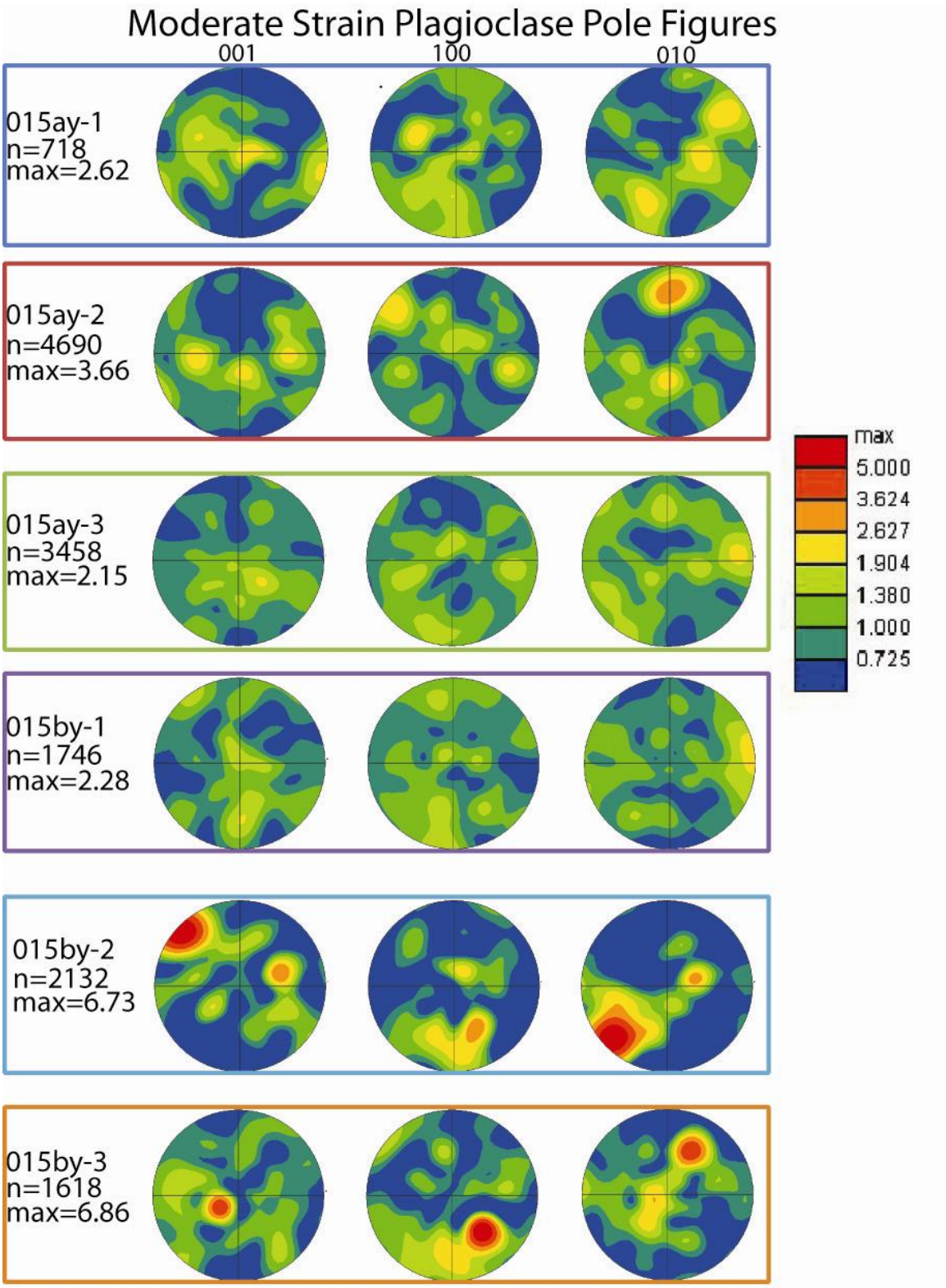

Figure 16. Moderate strain plagioclase pole figures of crystallographic orientation, showing absent to very weak CPO. See text and figure 14 for more details.

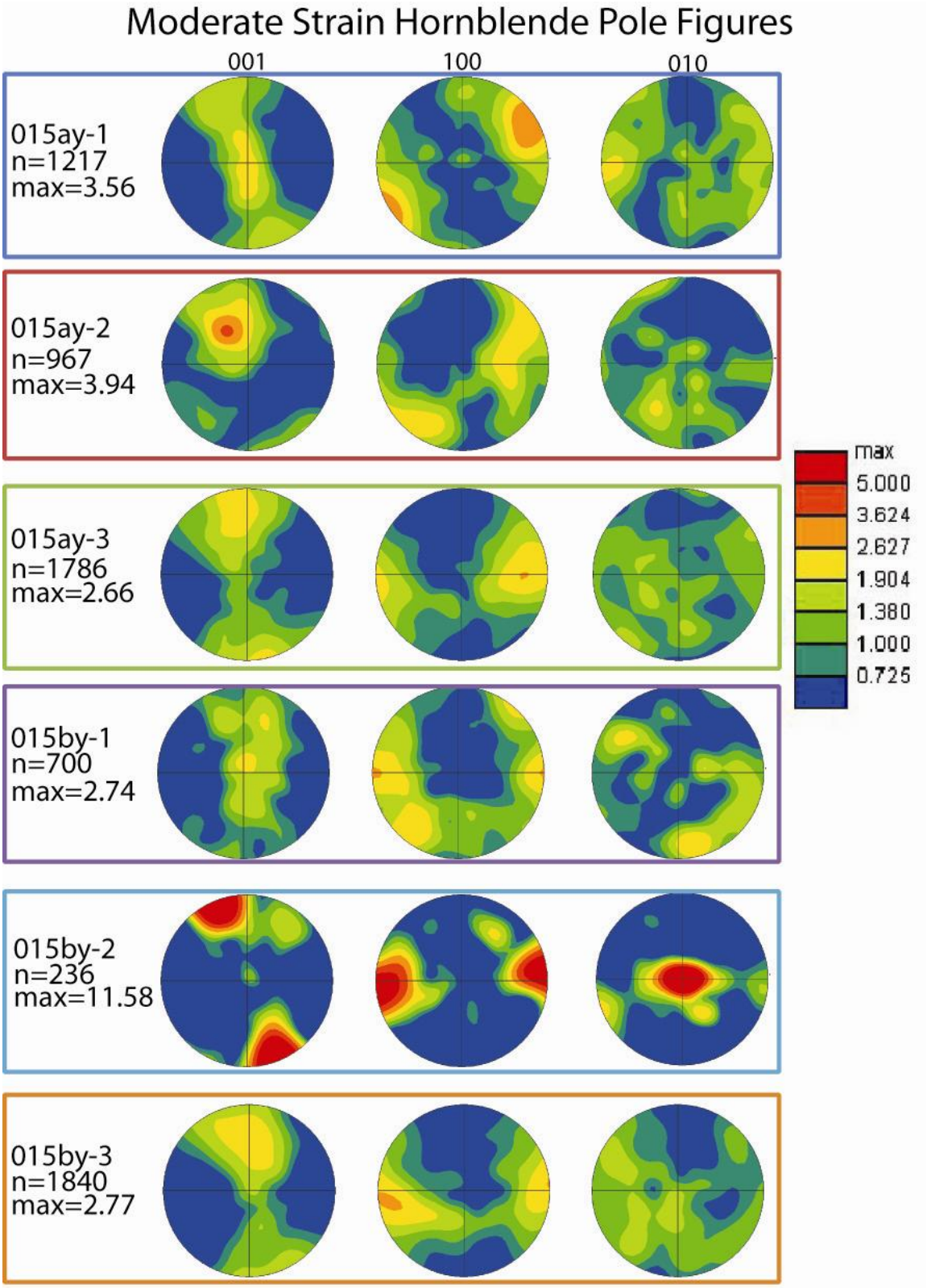

Figure 17. Moderate strain hornblende pole figures of crystallographic orientation, showing general alignment of the c-axes in the plane of foliation. Note that 015by-2 does not have a statistically significant number of grains. See text and figure 14 for more details.

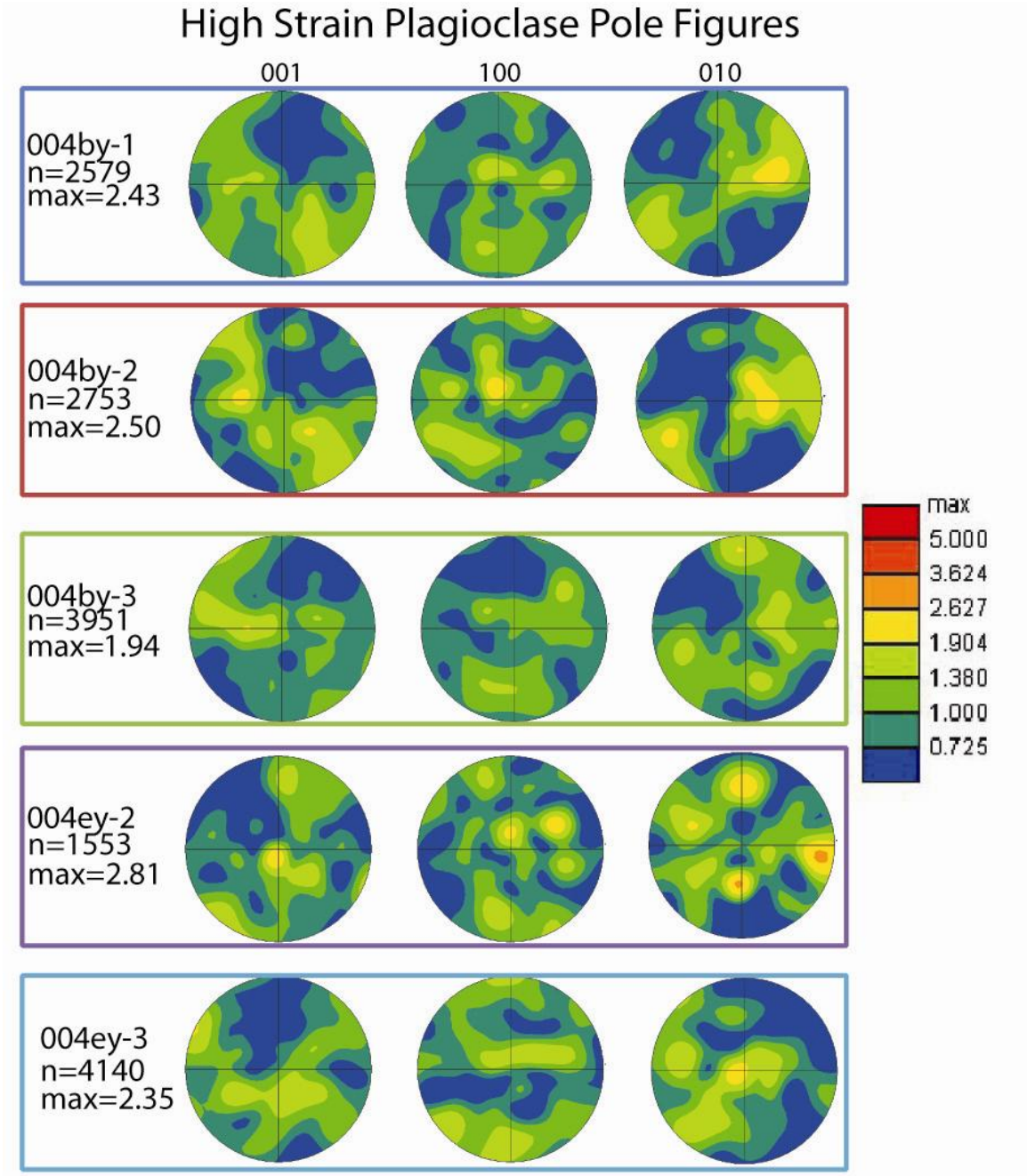

Figure 18. High strain plagioclase pole figure of crystallographic orientation of major axes. High strain samples have the greatest CPO for plagioclase but this is still very weak. See text and figure 14 for more details.

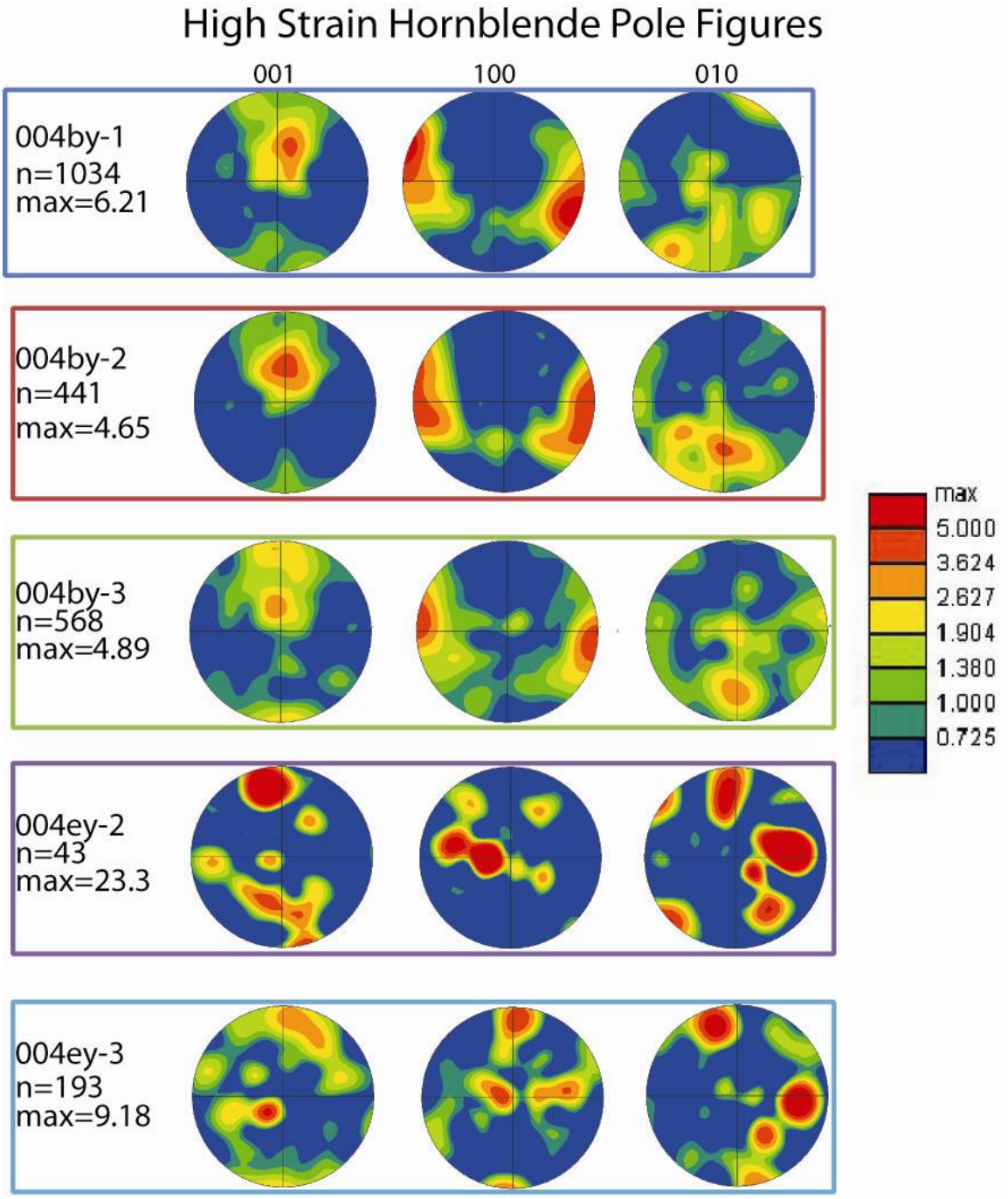

Figure 19. High strain hornblende pole figures of crystallographic orientation, showing a lineation of the c-axes in the plane of foliation. Note that 004ey-2 and 004by-3 do not have a statistically significant number of grains. See text and figure 14 for more details.

6. Shape Preferred Orientation

In low strain samples plagioclase is generally large and euhedral to subhedral. The recrystallized grains in high and moderate strain are generally tabular to polygonal. Hornblende is large and has a non-distinct shape in low strain. In high and moderate strain samples, grains are most commonly smaller, elongate and rhombohedral though they sometimes appear more tabular and similar to plagioclase.

SPO exists in the high, moderate and low strain samples for both hornblende and plagioclase. For plagioclase at all strain levels, major axis orientations range from 30° to 50° symmetrically about foliation. (Note, in SPO figures, the plane of foliation is at 90˚ on the graph.) In both hornblende and plagioclase low strain ellipse orientations are most uniform and consistent between sample areas, whereas moderate strain is more scattered (Figure 20). For both hornblende and plagioclase there is one orientation peak that is higher, to the 'right' of foliation. For hornblende in high strain samples the mode in ellipse orientation is between 10° and 30° oblique to foliation. Moderate and low strain samples are similar to each other in that they both have the same general shape for hornblende and two apparent orientation modes, both symmetrically about 30° to 50° to foliation (Figure 21).

In all of these, there are very few grains oriented parallel to foliation. One might expect that this is because of error in the methods used to calculate these statistics, but this in fact holds true on optical inspection of the thin sections. Hornblende grains, which define the foliation, are usually at least a few degrees offset from the foliation plane.

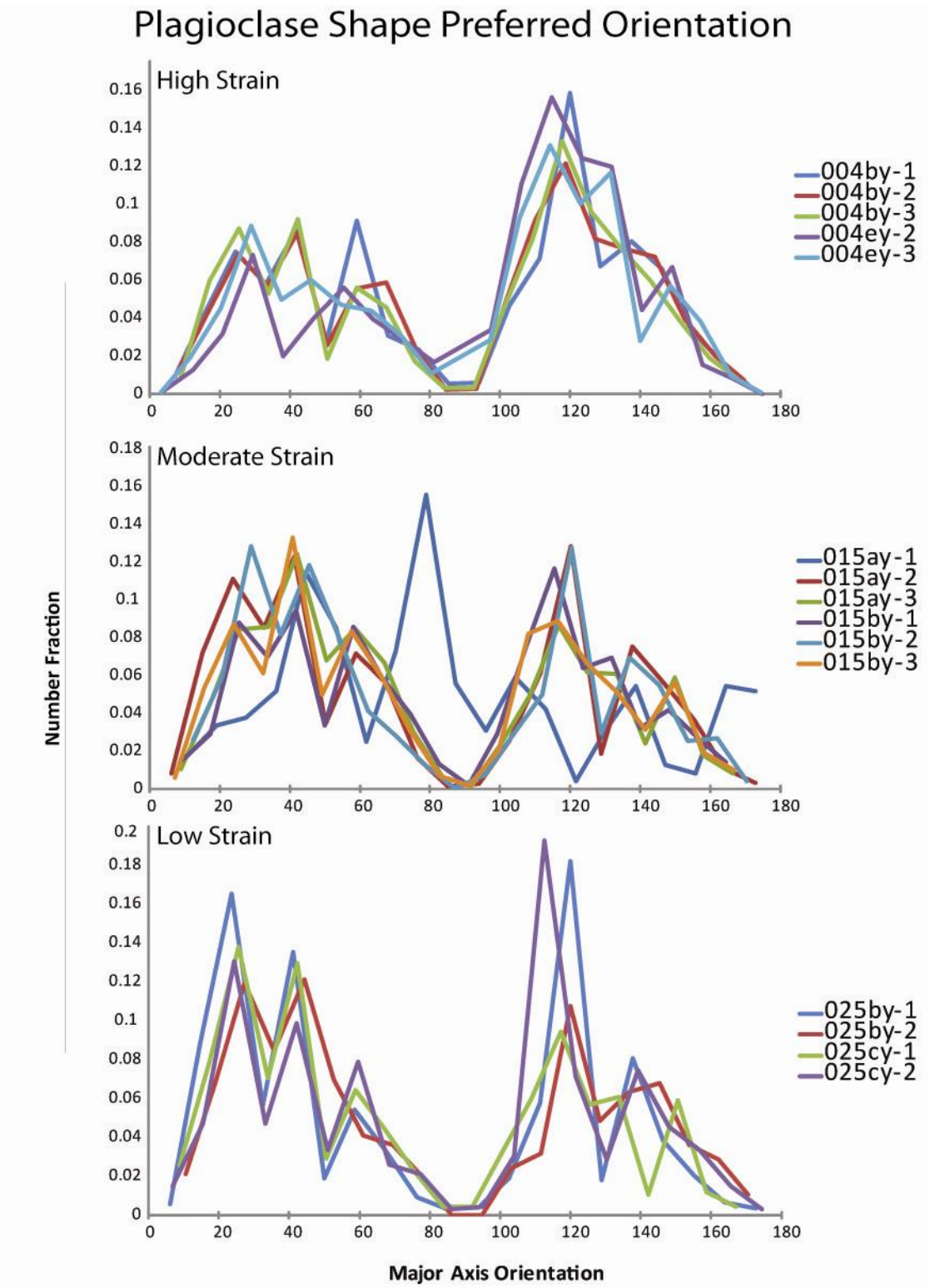

Figure 20. Plagioclase shape preferred orientation data. Plagioclase long axes are generally oblique to foliation by 30-50 degrees. SPO is somewhat uniform for plagioclase across the degrees of strain. See text for more details.

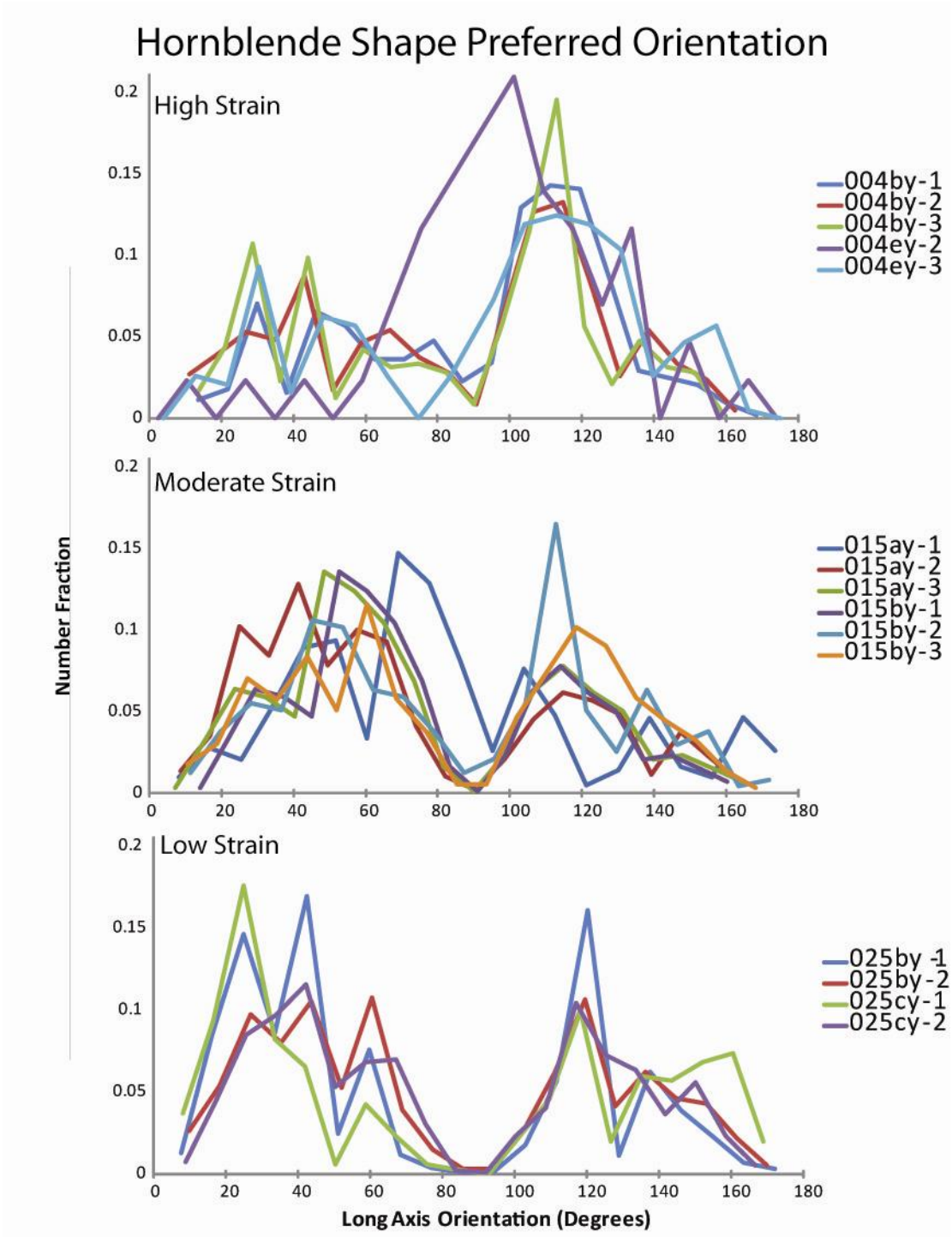

Figure 21. Shape preferred orientation for hornblende. The long axes of hornblende grains are commonly 20-50 degrees oblique to foliation. The grains from high strain samples are on average less oblique to foliation and have a stronger SPO. See text for more details.

7. Mineral Modes

The major mineral constituents of my samples are hornblende and plagioclase feldspar. Additionally, biotite, titanite, pyrite, calcite and tourmaline occur in minor quantities. In several thin sections biotite makes up as much as 5% of the sample, but in some samples (including high strain samples) it is absent. The others are accessory minerals and make up less than 1% of the section in most cases. Biotite doesn't appear to be significant in terms of rock strength. There is some variation in the mineral modes between different samples but the dominance of hornblende and plagioclase is consistent between samples and there are no other major minerals.

	Plagioclase (%)	Hornblende (%)
004by	80	19
004ey	87	13
015ay	65	35
015by	76	24
025by	64	36
025cy	75	25

Table 1- Mineral modes of plagioclase and hornblende from all of analyzed thin sections.

The proportion of hornblende varies from ~13% to ~36% between the samples and that of plagioclase varies from 64% to 87%. Consistently there is more plagioclase than hornblende in these rocks. The proportion of hornblende and plagioclase is very similar in moderate and low strain rocks, but there is slightly less hornblende in moderate strain samples. There is distinctly less hornblende in the high strain samples where it ranges from 13-19% of the section.

8. Mineral Chemistry

Plagioclase in these samples varies from An_{63} to An_{93}, and shows a trend towards more alkali composition with increasing strain (Figure 22). High strain samples have a broader range of An content than do low strain samples, ranging from 63% to 85%. Moderate strain samples range from An_{75} to An_{89} and low strain ranges from An_{78} to An_{94}. Generally, higher strain plagioclase is more rich in sodium and potassium. Also, plagioclase chemistry ranges have a great deal of overlap between the strain grades.

Hornblende chemistry has much less overlap between strain grades than plagioclase (Figure 22). Its composition ranges from $Si_{6.4}$ to $Si_{7.2}$ and $(Na+K)_{0.25}$ to $(Na+K)_{0.6}$. When silica and alkali content are plotted, hornblende does not seem to exhibit a chemical trend or evolution relating to strain; the high strain samples have intermediate alkali and silica contents between moderate and high strain samples. Plotting calcium and alkali content of hornblende we find that calcium content is generally low in the low strain rocks and high in the moderate and high strain rocks. High and moderate strain samples have significant overlap when plotted this way. Still hornblende does not show a distinct trend in its chemistry relating to strain.

9. Grain Aspect Ratios

Within each strain level, hornblende and plagioclase have similar grain aspect ratio distributions, which means that the aspect ratios of both minerals are similar in each sample (Figure 23 and 24). Consistently, across all the strain grades and for both

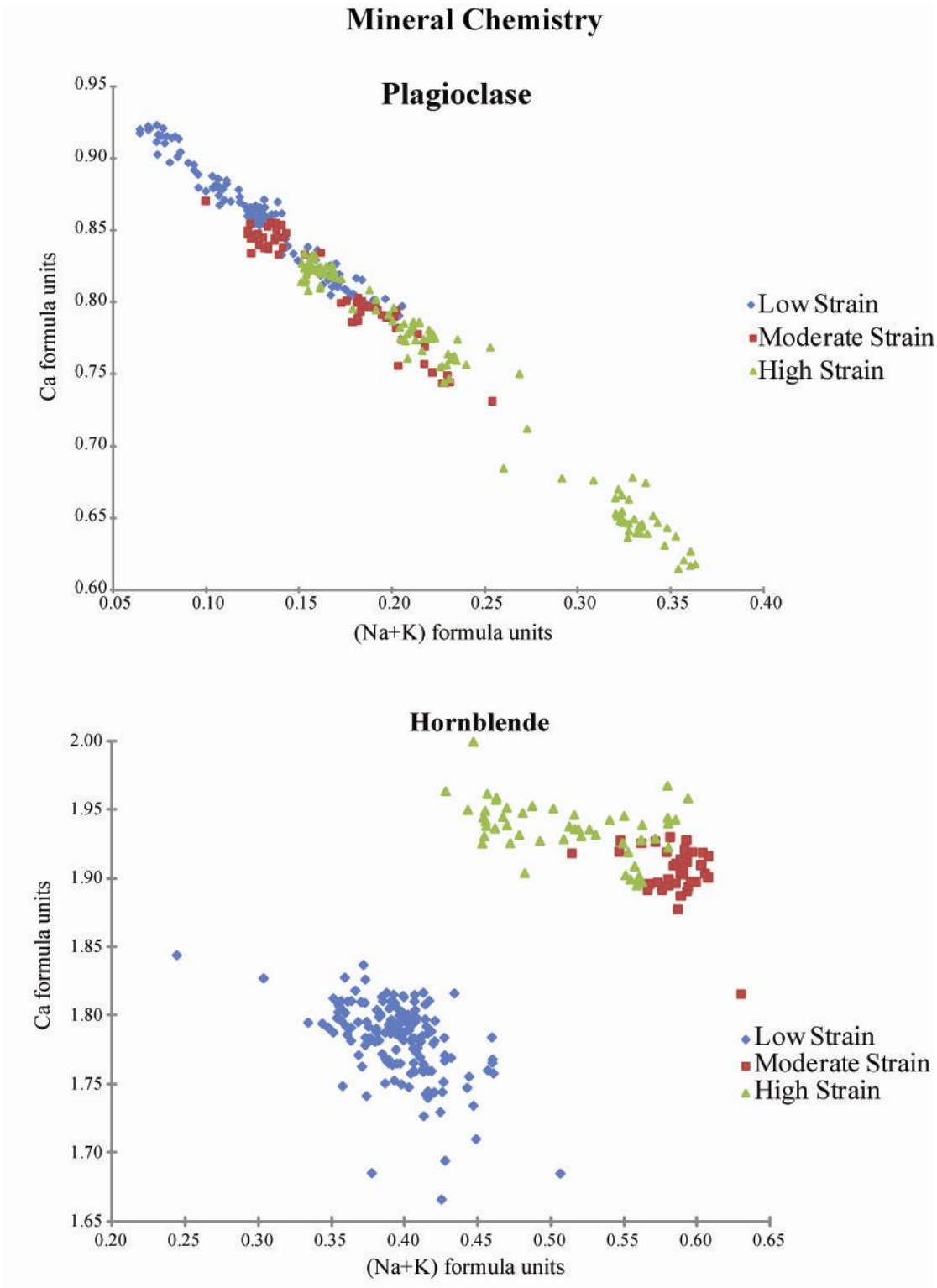

Figure 22. Select mineral chemistry plots for plagioclase and hornblende. Calcium and sodium plus potassium formula units are show for both mienrals. Plagioclase shows trend towards less calcic composition with higher strain and higher strain hornblende is more calcium rich.

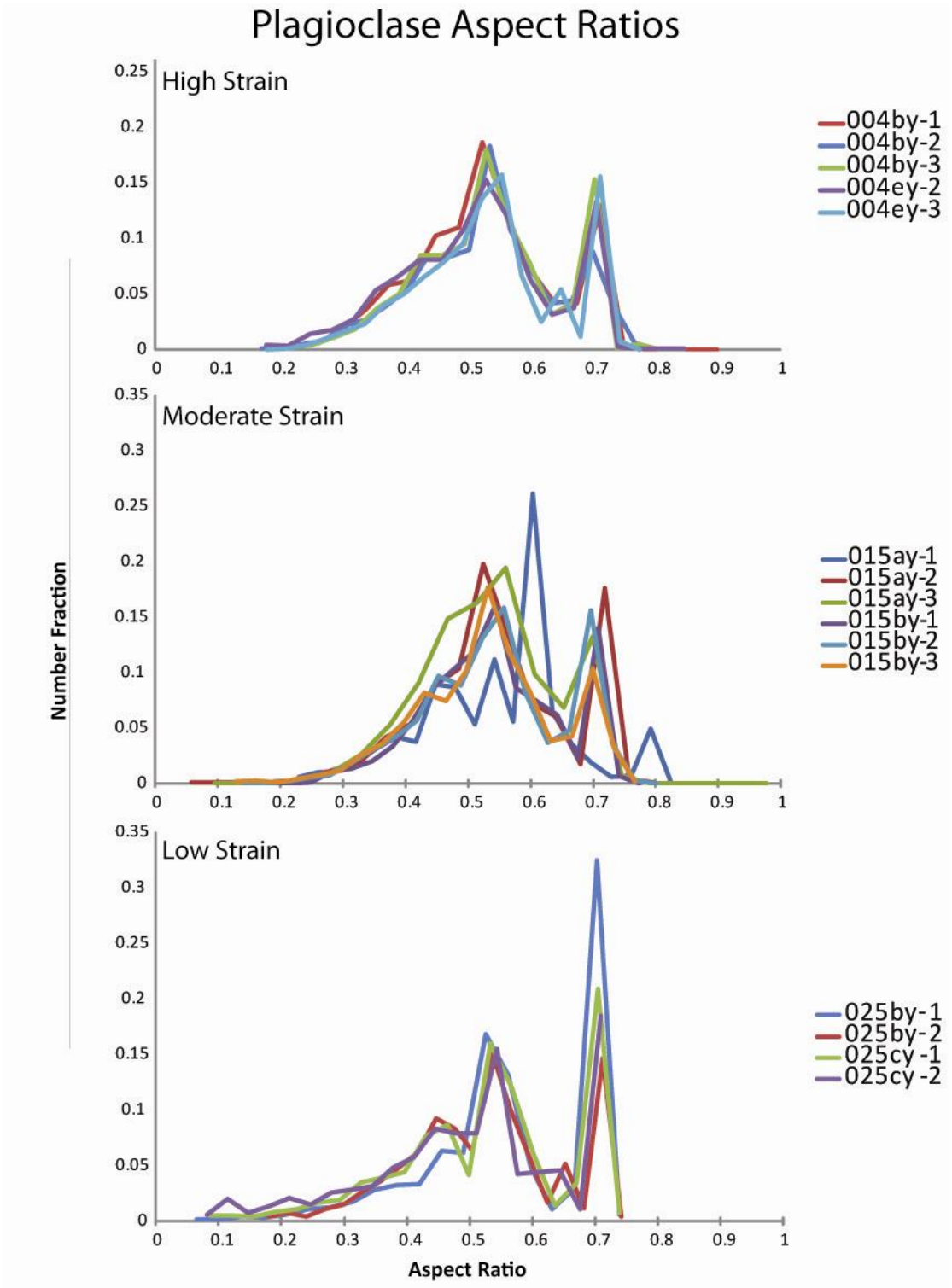

Figure 23. Plagioclase aspect ratio distributions. There are consistent peaks at about .52 and 7 though these vary in height with strain. Generally aspect ratios are greater (grains are more elongate) in higher strain. Note the similarity to hornblende aspect ratios. See text for more details

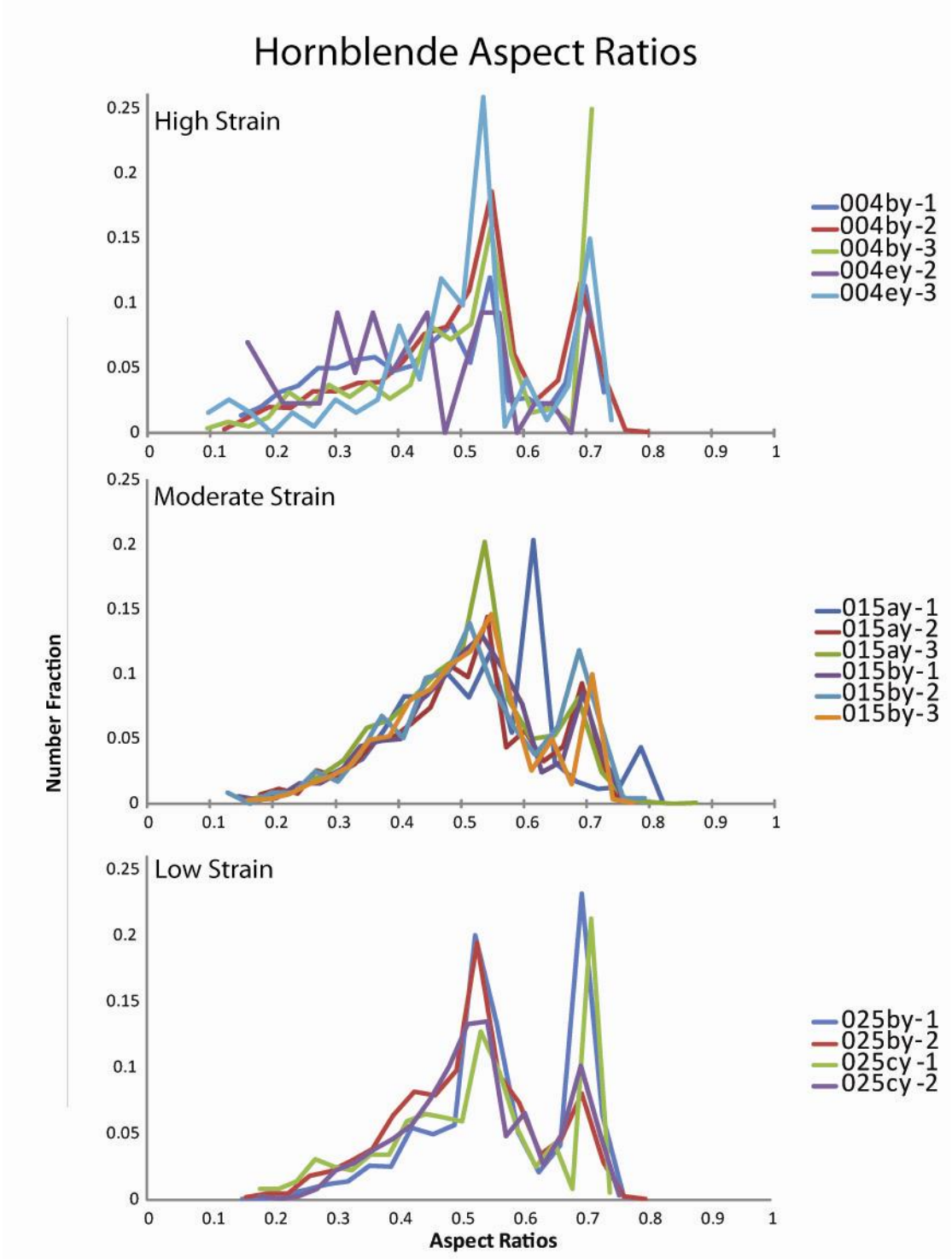

Figure 24. Hornblende aspect ratio distributions. There are consistent peaks at about .52 and 7 though these vary in height with strain. Generally aspect ratios are greater (grains are more elongate) in higher strain. Note the similarity to plagioclase aspect ratios.

minerals, there are two peaks in aspect ratio at about .52 and .7 (short/long axis). In high strain samples aspect ratios are generally lower for both plagioclase and hornblende, meaning that grains are more elongate. Lower strain samples have aspect ratios that are closer to one (i.e. grains are more equant).

10. Results Summary

With increasing strain these rocks exhibit progressively more pervasive grain size reduction and recrystallization. Plagioclase composition is increasingly more alkalic in higher strained rocks and hornblende does not seem show a chemical evolution though the composition is distinctly different between high, moderate and low strain rocks. Hornblende develops a strong CPO in moderate and high strain rocks and plagioclase shows a very weak CPO in high strain rocks. SPO is fairly consistent across the strain gradient for both plagioclase and hornblende. Refer to Table 2.

		High Strain	Moderate Strain	Low Strain
Texture	Plag	Almost entirely recrystallized, rare large grains	Large grains and recrystallized matrix	Almost completely large grains, small recrystallized patches
	Hbde	Defines gneissic banding	Dismembered and smeared out grains	Large, un-dismembered grains
Grain Size	Plag	Peak at 100-200μm	Peaks at 100-200μm and >500μm	>500μm
	Hbde	scattered distribution, most >200μm	ill-defined peak at 100-200μm	>500μm and minor peak at 100-200μm
CPO	Plag	Very weak c-axis alignment in plane of foliation	No preferred orientation	no preferred orientation
	Hbde	Strong c-axis lineation, b-axis perp. to foliation	Strong c-axis alignment in foliation plane, b-axis perp. to foliation	no preferred orientation
SPO	Plag	Two peaks 30-40˚ oblique to foliation, one stronger	Two peaks 30-40˚ oblique to foliation	Two peaks 30-40˚ oblique to foliation
	Hbde	Single peak 20-30˚ oblique to foliation	Two peaks 20-30˚ oblique to foliation	Two well defined peaks 20-30˚ oblique to foliation
Mineral Mode	Plag	80-87%	65-76%	64-75%
	Hbde	13-19%	24-35%	25-36%
	Biotite	~5% to absent	<5% to absent	Not present
Chemistry	Plag	An_{63} to An_{85}, widely spread bimodal distribution	An_{75} to An_{89}, bimodal distribution	An_{78} to An_{93}, unimodal distribution
	Hbde	Moderate silica and alkali content, wide distribution	High alkalis and low silica, concentrated distribution	Lowest silica and alkali, concentrated distribution
Aspect Ratios	Plag	Similar ratios for hbde and plag, higher aspect ratios	Moderate aspect ratios, but not hugely different from other samples	Lowest aspect ratios
	Hbde	Higher aspect ratios, peaks are consist for both minerals for all samples	Moderate aspect ratios, not different from other samples	Lowest aspect ratios

Table 2. Summary of the results of my EBSD, WDS and optical analysis. See text formore details.

INTREPRETATIONS AND MINERAL DEFORMATION MECHANISMS

1. Hornblende

In the middle crust hornblende usually deforms by brittle fracturing and grain boundary sliding below temperatures of about 650˚C (Berger and Stunitz 1996, Imon et al. 2004). However, ShuYun et al. (2007) note that this is close to the brittle/ductile transition of hornblende. In most cases plastic deformation has only been noted in rocks that have experienced deformation during granulite grade metamorphism (Edydio-Silva et al. 2002) and in experimentally deformed rocks (Berger and Stunitz 1996). Dislocation creep microstructures are more common under such conditions, but in cases where abundant fluids are present diffusion creep has been observed (Diaz Aspiroz et al. 2007). Generally, hornblende is rheologically strong relative to other minerals in the middle and lower crust (Diaz Aspiroz et al. 2007).

Hornblende grains in my rocks are cracked, dismembered and displaced with no features that suggest internal strain (Figure 11-3). All of these observations are indicative of brittle fracturing and cataclastic flow of hornblende rather than plastic flow and dislocation creep (Passchier and Trouw, 2005). I did not observe any evidence of subgrain formation, undulating extinctions, twinning or other microstructures that would suggest plastic deformation. The interpretation that hornblende is deforming by brittle fracture is consistent with other work on rocks under similar conditions (Diaz Aspiroz et al. 2007, Berger and Stunitz 1996).

Rigid body rotation of hornblende grains in a viscous matrix can lead to the development of a CPO (Berger and Stunitz 1996). With a stronger SPO one would expect a stronger CPO because the shape of a hornblende grain is commonly defined by crystallographic cleavage planes (Berger and Stunitz 1996, Diaz Aspiroz et al. 2007). A strong CPO exists for hornblende in my high and moderate strain samples and a definite SPO exists in my high strain samples, but it is not particularly strong (Figure 15, 17 and Figure 21). Imon et al. (2004) suggests that cataclasis only develops a weak CPO from an SPO and furthermore that dissolution precipitation creep may contribute once grains are fractured and fluids become more mobile.

In one case, Imon et al. (2004) found that green hornblende (more Ca-rich) was being precipitated on brown hornblende. There is no distinct color zonation in my samples and microprobe analysis did not yield any notable chemical zonation. However there seems to be a evolving trend of calcium loss by plagioclase with increasing strain and increased calcium in high and moderate strain hornblende (Figure 22). This is suggestive of a diffusive reaction between plagioclase and hornblende, which may have taken the form of diffusion creep. Hornblende however does not show a chemical evolution as plagioclase does; there is not a continuous chemical trend in hornblende composition. This fact may indicate that the composition of hornblende within the outcrop was original heterogeneous before deformation occurred. Hornblende in these rocks has certainly deformed by brittle fracturing which may have been followed by diffusion creep when fluids were available. Diffusion reactions as well as original differences in the chemistry over the space of the outcrop contribute to the chemical trends that I observe.

2. Plagioclase

Deformation mechanisms for plagioclase are not well understood or widely studied for reasons of technical difficulty (Xie et al. 2003). It is likely that microfracturing and cataclastic flow play a role in the deformation of plagioclase (Tullis and Yund 1987). Dislocation creep has been observed in plagioclase of lower granulite facies rocks in the form of subgrain rotation recrystallization (Olsen and Kohlstedt 1984). The development of a CPO in deformed plagioclase has been attributed to geometric rotation or anisotropic growth processes at lower temperatures and dislocation glide, mechanical twinning and dynamic recrystallization at high temperature (Xie et al. 2003 and sources therein).

Based on my observations, plagioclase textures indicate that it has mostly deformed by dislocation creep in the form of subgrain rotation, which seems to initiate along fractures in large plagioclase grains. This can be seen in the occurrence of small, clean subgrains along fractures and grain boundaries (Figure 11-1). However, despite microstructural evidence, plagioclase does not exhibit the CPO commonly associated with dislocation creep. Based on previous work (Xie et al. 2003), one would expect a stronger CPO in plagioclase that has experience simply dislocation creep, but in fact plagioclase CPO even in high strain samples is weak at best.

Recovery processes may have lead to plagioclase CPO being erased or overprinted in these rocks, which would explain why there is only a slight CPO in high strain samples. It is possible that as grain size has been reduced, these rocks have experienced a switch from grain-size-insensitive dislocation creep, to grain-size-sensitive

diffusion creep. With a reduction in grain size, diffusion creep becomes more dominant (Bercovici and Karato 2003). Rybacki and Dresen (2003) have proposed that diffusion creep may dominate under a wide range of deformation conditions and is especially dominant for wet feldspar. The crystallographic orientation patterns that are observed could be a result of initially dominant dislocation creep which was then overtaken by diffusion creep with the addition of fluids and grain size reduction. As noted above, diffusion processes are likely to have acted in these rocks given the chemical trends that I have observed.

These conclusions are at odds with the work of De Bresser et al. (2001) who suggests that a switch from grain-size-insensitive creep to grain-size-sensitive creep is unlikely because recovery processes will prevent it. In any case, it is clear from observed textures that microfracturing, recovery and probably dislocation creep have occurred in plagioclase in my samples. Diffusion creep may have dominated at some point but there is no clear evidence of this. Crystallographic orientation data remains somewhat ambiguous in terms of deformation mechanisms of plagioclase.

3. Recovery

It seems that these rocks have had time at depth to undergo static recrystallization and recovery. This is evident from the 120 degree triple junctions observed in small plagioclase grains and in many hornblende grains. This 120 degree relationship is less prominent when there is an abundance of small hornblende grains interspersed with

plagioclase grains (Figure 11-3). Hornblende grains may pin and inhibit grain growth of plagioclase associated with recovery.

4. Relative Strength of Plagioclase and Hornblende

One fundamental question of this research is: which is weaker- hornblende or plagioclase? If hornblende is acting as the weak phase in these rocks, whether or not the grains are linked up or isolated will affect the weakness of the rock. But hornblende interconnectedness seems unrelated to strain, implying that hornblende is not the weaker phase. Conversely, if grain size reduced areas of plagioclase are truly weaker, then whether or not these areas are interconnected could play a role in rock weakening (Figure 11-2). In fact, in high and moderate strain samples zones of recrystallized plagioclase are more interconnected and pervasive.

Low strain samples have disconnected patches of recrystallized plagioclase; in moderate strain recrystallized plagioclase is interconnected through the samples but many large grains remain; and in high strain recrystallization of plagioclase is almost completely pervasive. Hornblende is almost always broken up when plagioclase is recrystallized. This seems logical because if hornblende is stronger and resisting strain it has to break before recrystallization of plagioclase can take place. Interconnectedness of a weak phase is widely recognized as a fundamental characteristic relating to rock strength (Handy 1994, Holyoke and Tullis 2006). If there is a framework of stronger minerals the rock will be much stronger than if the weak phase is interconnected. It

seems to be the case in my rocks that hornblende is the stronger mineral and plagioclase is the weaker.

WEAKENING MECHANISMS

Given the microstructural analysis that I have performed, I can rule out several of the weakening and localization mechanisms mentioned in the background section. Melt formation can be ruled out from the lack of evidence in thin section and improper conditions for formation. The temperature and pressure conditions are not great enough to produce melt. Also, given the small size of these shear zones it is unlikely that there was enough of a temperature gradient across this space to cause localization and I am unaware of any nearby intrusive bodies, thus thermal perturbations are unlikely. Shear heating (falling under the category of thermal perturbations) is one mechanism I cannot rule out based on the work I have done. Determining the influence of shear heating would involve calculations which I have not performed. It is possible that as shearing increased these rocks became hotter resulting in further localization though I have no evidence for this. Reaction related weakening, in the form of metasomatism or metamorphic phase changes, is not likely to have had an effect because the bulk mineralogy is fairly consistent across the strain gradient. There is not addition of weaker minerals or subtraction of strong minerals by mineral reactions.

There are several possible mechanisms by which these rocks may have been locally weakened leading to strain localization. The introduction of fluids, resulting in hydrolytic weakening, is one possibility. In the Central Metasedimentary Belt and CMBbtz, fluids have likely been available over a long time period (Grittins 1961 and Marshall 2012). The presence of biotite in high and moderate strain samples is somewhat suggestive of the presence of water in these rocks because it is a hydrous

phase. It appears that fracturing has played a role in recrystallization of plagioclase and hornblende and is thus ubiquitous in these rocks. These fractures may have provided a route of entrance for fluids to interact with these rocks and weaken them.

Also, there are a few small veins within this outcrop, which appear to be syn-deformational, and which may have provided a nearby source of fluids. Fluid related weakening is possible, though I do not have direct microstructural or chemical evidence to suggest how significant it might have been. These veins are commonly associated with shear zones and often occur at the center of a highly strained zone. This observation, by association, suggests that veins and associated processes have had some role in localizing strain. Due to a lack of foresight in sampling I did not sample these veins for analysis to determine what influence they have had on the outcrop.

The presence of veins, in addition to supplying fluids, may have localized strain in a different way. A lithologic boundary or other kind of strength contrast may cause a reorganization of the stress field around that boundary such that stress is not equal throughout the material. If stress is heterogeneous, deformation can be concentrated were stress is greater. Veins cutting across this outcrop may concentrate stress in this way. Similarly we cannot rule out the possibility that stress has been concentrated in this outcrop by factors external to it. There may have been features of the surrounding rock that caused stress to be localized rather than uniformly stressing this body of rock that I have been examining.

The most probable changes and rock characteristics that led to weakening are related to texture. I will divide these into inherent and evolving textural characteristics. It is clear from the mineral modes that the proportions of hornblende and plagioclase vary

throughout this outcrop. There is distinctly more plagioclase in high strain rocks. This association, along with the fact that we know plagioclase to be the weaker mineral, leads me to believe that a high proportion of plagioclase within the outcrop could lead to strain localization.

Also the interconnectedness of plagioclase as the weak phase, preventing hornblende from providing a strong framework, may have localized strain (Handy 1994). This is evident from the interconnectedness of the recrystallized plagioclase in the moderate strain samples. Larger scale strain does not seem to occur when recrystallized plagioclase is isolated as in the low strain rocks. Both of these inherent heterogeneities in this outcrop are possible, especially if there had been magmatic flow as this rock crystallized which may have aligned plagioclase grains or sorted the minerals into a heterogeneous distribution.

As deformation continues, both hornblende and plagioclase can texturally evolve to become progressively weaker. Brittle fracturing of hornblende leads to greater ease of fluid infiltration and an increasing dominance of diffusion creep which is a faster creep mechanism (Imon et al. 2004). As noted above it is possible that as plagioclase grain size was reduced, a switch in the dominant creep mechanism to diffusion creep may have occurred which would also lead to decreased rock strength. Diffusion reactions are evident from the chemical trends of calcium and sodium in plagioclase and hornblende. Both of these processes would progressively weaken the rock as deformation continues. Though these processes may not initially localize strain they could have lead to progressively greater strain in this outcrop.

CONCLUSIONS

I have examined an outcrop of anorthositic gabbro rock from the Salerno Creek deformation zone of the Central Metasedimentary Belt boundary thrust zone in the Grenville province of southern Ontario. The SCDZ may be a significant lithotectonic boundary in terms of the evolution of this region of Grenville orogen. The outcrop of my research rapidly grades from relatively unstrained to highly strained over a small space in multiple meter to centimeter scale shear zones. To examine the mechanisms of strain localization in this instance I have sampled low, moderate and highly strained rock to compare the rock's characteristics across the strain gradient. I have measured grain size, CPO, SPO, grain aspect ratios and mineral chemistry for the primary minerals, hornblende and plagioclase, in this rock.

From my study, I can conclude several things about the deformation and weakening mechanisms that have acted on these rocks. Hornblende deformed primarily by brittle fracturing as demonstrated by microstructural features. As fracturing progressed, making fluids more mobile, diffusion creep processes may have played a more significant part. These interpretations are supported by the strong CPO and SPO along with mineral chemistry data. Plagioclase deformed by dislocation creep in the form of subgrain rotation recrystallization with a possible switch to diffusion creep with decreasing grain size. Subgrain formation of plagioclase commonly localizes along intergranular fractures.

The most important factors controlling rock strength and strain localization in this outcrop are related to textural heterogeneities and changes. Plagioclase is the weaker

mineral in this rock so the degree to which it is interconnected will greatly influence rock strength. I have found that in higher strain rocks areas of plagioclase recrystallization become increasingly interconnected. Also, the proportion of plagioclase in high strain rocks is greater, which is consistent with the bulk rock being weaker. Both plagioclase interconnectedness and varying proportions of minerals may be characteristics inherent to the body of rock before deformation. As deformation progresses both plagioclase and hornblende can become progressively weaker and further localize strain.

The presence of fluids and veins is also important. Fluids are abundant in this region and can enter through fractures to readily weaken rocks. The veins in this outcrop may have supplied fluids, allowing strain to localize and they also may have concentrated stress if their strength is in contrast to the surround outcrop. I also cannot rule out the possibility that stress concentration may have been controlled by factors outside of this outcrop and in the surrounding region.

REFERENCES

Barshi, N. A., 2012, Conflicting Kinematics of the Salerno Creek Deformation Zone, Grenville Province, Ontario: Northampton, MA, Unpub. A.B. Honors Thesis, Smith College, 59 p.

Bercovici, D., and Karato, S., 2003, 13 Theoretical Analysis of Shear Localization in the Lithosphere, in Karato, S., Wenk, H., eds., Reviews in Mineralogy and Geochemistry: Plastic Deformation of Minerals and Rocks, v. 51, Chpt.3, p. 387-421.

Berger, A., and Stunitz, H., 1996, Deformation mechanisms and reaction of hornblende□: examples from the Bergell tonalite (Central Alps): Tectonophysics, v. 257, p. 149-174.

Carr, S.D., Easton, R.M., Jamieson, R.A., and Culshaw, N.G., 2000, Geologic transect across the Grenville orogen of Ontario and New York 1: Moon, v. 216, p. 193-216.

Crameri, F., and Kaus, B.J.P., 2010, Parameters that control lithospheric-scale thermal localization on terrestrial planets: Geophysical Research Letters, v. 37, no. 9, p. 1-6, doi: 10.1029/2010GL042921.

Davis, G., and Reynolds, S., 1996, Structural Geology of Rocks and Regions: United States of America, John Wiley & Sons, Inc., 199 and 509 p.

Díaz Aspiroz, M., Lloyd, G.E., and Fernández, C., 2007, Development of lattice preferred orientation in clinoamphiboles deformed under low-pressure metamorphic conditions. A SEM/EBSD study of metabasites from the Aracena metamorphic belt (SW Spain): Journal of Structural Geology, v. 29, no. 4, p. 629-645, doi: 10.1016/j.jsg.2006.10.010.

Easton, R.M., and Kamo, S.L., 2011, Harvey-Cardiff domain and its relationship to the Composite Arc Belt, Grenville Province: insights from U–Pb geochronology and geochemistry: Canadian Journal of Earth Sciences, v. 48, no. 2, p. 347-370, doi: 10.1139/E10-064.

Egydio-Silva, M., Vauchez, A., Bascou, J., and Hippertt, J., 2002, High-temperature deformation in the Neoproterozoic transpressional Ribeira belt, southeast Brazil: Tectonophysics, v. 352, no. 1-2, p. 203-224, doi: 10.1016/S0040-1951(02)00197-X.

Gerace-Fowler, N., 2012, Thermobarometric evidence for a common central metasedimentary belt affinity of the Bancroft and Elzevir terranes, Ontario, Canada: Proceedings of the 24th Annual Keck Research Symposium in Geology, (in press).

Grittins, J., 1961, Nephelinization in the Haliburton-Bancroft District , Ontario , Canada: The Journal of Geology, v. 69, no. 3, p. 291-308.

Hanmer, S., Corrigan, D., Pehrsson, S., and Nadeau, L., 2000, SW Grenville Province , Canada□: the case against post – 1 . 4 Ga accretionary tectonics: Geographical, v. 319, p. 33-51.

Hanmer, S., and McEachern, S., 1992, Kinematic and rheological evolution of a crustal-scale ductile thrust zone, Central Metasedimentary Belt, Grenville orogen, Ontario: Canadian Journal of Earth Sciences, v. 29, p. 1779-1790.

Holyoke, C.W., and Tullis, J., 2006, Mechanisms of weak phase interconnection and the effects of phase strength contrast on fabric development: Journal of Structural Geology, v. 28, no. 4, p. 621-640, doi: 10.1016/j.jsg.2006.01.008.

Imon, R., Okudaira, T., and Kanagawa, K., 2004, Development of shape- and lattice-preferred orientations of amphibole grains during initial cataclastic deformation and subsequent deformation by dissolution–precipitation creep in amphibolites from the Ryoke metamorphic belt, SW Japan: Journal of Structural Geology, v. 26, no. 5, p. 793-805, doi: 10.1016/j.jsg.2003.09.004.

Kirby, S., 1985, Rock mechanics pertinent to the rheology of the continental lithosphere and the localization of strain along shear zones, Tectonophysics, v. 119, p. 1-27.

Kronenberg, A., Segall, P., Woolf, G., 1990. Hydrolytic weakening and penetrative deformation within a natural shear zone. In: The Brittle Ductile Transition in Rocks (eds. A. Duba, W. Durham, J. Handin, H. Wang), Geophysical Monograph 56, p. 21-37.

Lumbers, S., and Vertolli, V., compilers, Precambrian Geology, Gooderham Area003A Ontario Geology Survey, Preliminary Map, P.3405, scale 1:50,000.

Mancktelow, N.S., and Pennacchioni, G., 2005, The control of precursor brittle fracture and fluid–rock interaction on the development of single and paired ductile shear zones: Journal of Structural Geology, v. 27, no. 4, p. 645-661, doi: 10.1016/j.jsg.2004.12.001.

Marshall, E., 2012, Petrology and Geochemistry of the Allsaw Anorthosite: A scapolitized meta-anorthosite in the Grenville Province, Ontario: Proceedings of the 24th Annual Keck Research Symposium in Geology, (in press).

McLelland, J.M., Selleck, B.W., and Bickford, M.E., 2010, Review of the Proterozoic evolution of the Mesoproterozoic inliers of the Appalachians: Geological Society Of America Memoirs, doi: 10.1130/2010.1206(02).

Miller. R., and Lentz, D., 2003, Kinematic and rheological evolution of a crustal-scale ductile thrust zone, Central Metasedimentary Belt, Grenville orogen, Ontario: Discussion, Canadian Journal of Earth Sciences, v. 30, p. 647-649.

Misra, S., Burlini, L., and Burg, J., 2009, Strain localization and melt segregation in deforming metapelites: Physics of the Earth and Planetary Interiors, v. 177, no. 3-4, p. 173-179, doi: 10.1016/j.pepi.2009.08.011.

Montanye, B., 2012, Calcite-Graphite Thermometry: Proceedings of the 24th Annual Keck Research Symposium in Geology, (in press).

Montesi, L.G.J., and Zuber, M.T., 2002, A unified description of localization for application to large-scale tectonics: Journal of Geophysical Research, v. 107, no. B3, p. 1-21.

Nesbit, J., 2012, Calcite-Graphite Thermometry in the Southwesternmost Central Metasedimentary Belt, Grenville Province, Southern Ontario: Proceedings of the 24th Annual Keck Research Symposium in Geology, (in press).

Olsen, T., and Kohlstedt, D., 1984, Analysis of dislocations in some naturally deformed plagioclase feldspars: Physics and Chemistry of Minerals, v. 11, p. 153-160.

Ontario Geological Survey, 1991. Bedrock geology of Ontario, southern sheet: Ontario Geological Survey, Map2544,scale1:1,000,000.

Passchier, C., and Trouw, R., 2005, Microtectonics: 2nd Edition: New York, Springer, Berlin and Heidelberg, 26 p.

Rybacki, E., and Dresen, G., 2004, Deformation mechanism maps for feldspar rocks: Tectonophysics, v. 382, no. 3-4, p. 173-187, doi: 10.1016/j.tecto.2004.01.006.

ShuYun, C., Liu, J., and Hu, L., 2007, Micro-and submicrostructural evidence for high-temperature brittle-ductile transition deformation of hornblende: Case study of high-grade mylonites from Diancangshan, western Yunnan: Science in China Series D: Earth Sciences, v. 50, no. 10, p. 1459-1470, doi: 10.1007/s11430-007-0063-3.

Tullis, J., and Yund, R., 1987, Transition from cataclastic flow to dislocation creep of feldspar: mechanisms and microstructures: Geology, v. 15, no. 7, p. 606-609.

White, S.H., Burrows, S.E., Carreras, J., Shaw, N.D., and Humphreys, F.J., 1980, On mylonites in ductile shear zones: Journal of Structural Geology, v. 2, no. 1-2, p. 175-187, doi: 10.1016/0191-8141(80)90048-6.

Wintsch, R., Christoffersen, R., Kronenberg, A., 1995. Fluid-rock weakening of fault zones. Journal of Geophysical Research, Vol. 100, 13,021-13,032.

Wodicka, N., Ketchum, J.W.F., and Jamieson, R.A., 2000, Grenvillian metamorphism of monocyclic rocks, Georgian Bay, Ontario, Canada: Implications for convergence history: The Canadian Mineralogist, v. 38, no. 1998069, p. 471-510.

Xie, Y., Wenk, H.-R., and Matthies, S., 2003, Plagioclase preferred orientation by TOF neutron diffraction and SEM-EBSD: Tectonophysics, v. 370, no. 1-4, p. 269-286, doi: 10.1016/S0040-1951(03)00191-4.

APPENDICES

Below are all of the chemical analyses of plagioclase and that I performed during this research. Each row of data is from one specific point analyzed using the electron microprobe. The bold headings at the top of each column denote the element whose measurements are in that column. These data are formula units of each major element in plagioclase and hornblende. The thin sections that these analyses were gathered from are 025by, 015by, 004by which are low, moderate and high strain samples, respectively.

025by
Plagioclase

Na	K	Mg	Ca	Fe	Al	Si	Total
0.162	-0.001	-0.001	0.819	0.002	1.864	2.152	4.997
0.170	0.000	0.000	0.827	0.002	1.859	2.149	5.007
0.155	0.000	-0.001	0.838	0.001	1.852	2.153	4.999
0.157	0.000	-0.001	0.832	0.001	1.871	2.142	5.001
0.150	-0.001	-0.001	0.829	0.001	1.872	2.145	4.994
0.160	0.000	0.000	0.836	0.002	1.866	2.141	5.006
0.157	-0.001	0.000	0.831	0.001	1.876	2.139	5.001
0.159	0.000	-0.001	0.829	0.001	1.877	2.137	5.004
0.144	0.000	-0.001	0.839	0.002	1.870	2.142	4.995
0.143	0.000	0.000	0.844	0.002	1.879	2.132	4.999
0.163	0.000	-0.001	0.812	0.002	1.863	2.156	4.994
0.163	0.000	0.000	0.819	0.001	1.855	2.158	4.996
0.166	0.001	0.000	0.819	0.001	1.850	2.162	4.997
0.160	0.000	-0.001	0.823	0.001	1.856	2.156	4.996
0.171	0.001	-0.001	0.819	0.002	1.848	2.161	5.000
0.170	-0.001	-0.001	0.814	0.001	1.855	2.159	4.998
0.184	-0.001	-0.001	0.816	0.002	1.847	2.161	5.007
0.181	0.000	-0.001	0.817	0.002	1.838	2.168	5.004
0.175	-0.001	-0.001	0.809	0.002	1.848	2.166	4.997
0.171	0.000	-0.001	0.811	0.002	1.840	2.173	4.993
0.191	0.000	0.000	0.799	0.001	1.841	2.172	5.003
0.190	0.000	-0.001	0.801	0.002	1.828	2.181	5.000
0.191	-0.001	-0.001	0.802	0.002	1.830	2.178	5.002

0.196	0.000	-0.001	0.802	0.001	1.825	2.181	5.004
0.187	0.000	-0.001	0.798	0.002	1.837	2.175	5.000
0.186	0.000	-0.001	0.799	0.001	1.844	2.171	5.000
0.204	0.000	0.000	0.791	0.002	1.823	2.185	5.006
0.177	0.000	-0.001	0.803	0.001	1.845	2.170	4.995
0.205	0.000	-0.001	0.797	0.001	1.832	2.176	5.010
0.182	-0.001	0.000	0.790	0.001	1.852	2.171	4.994
0.169	0.000	-0.001	0.826	0.002	1.847	2.160	5.001
0.166	0.000	-0.001	0.816	0.001	1.861	2.155	4.997
0.179	0.001	-0.001	0.806	0.002	1.849	2.165	5.000
0.148	-0.001	-0.001	0.834	0.003	1.863	2.148	4.994
0.167	0.000	-0.001	0.825	0.002	1.860	2.150	5.003
0.168	-0.001	-0.001	0.805	0.001	1.854	2.165	4.991
0.170	0.001	-0.002	0.813	0.001	1.851	2.164	4.996
0.168	0.000	-0.001	0.811	0.001	1.851	2.164	4.994
0.175	0.001	-0.001	0.808	0.000	1.841	2.172	4.995
0.171	0.000	0.000	0.816	0.002	1.833	2.173	4.995
0.074	0.000	0.000	0.916	0.001	1.950	2.061	5.002
0.074	0.000	-0.001	0.911	0.002	1.956	2.058	5.001
0.075	-0.001	-0.001	0.903	0.000	1.959	2.062	4.996
0.077	0.001	-0.001	0.910	0.001	1.938	2.072	4.997
0.079	0.000	-0.001	0.915	0.001	1.942	2.066	5.002
0.086	-0.001	-0.001	0.914	0.000	1.944	2.065	5.006
0.076	0.000	-0.001	0.916	0.001	1.958	2.056	5.004
0.074	0.000	0.000	0.923	0.002	1.948	2.058	5.004
0.070	0.000	-0.001	0.921	0.000	1.942	2.067	4.997
0.065	-0.001	-0.001	0.917	0.000	1.948	2.064	4.994
0.107	0.000	-0.001	0.867	0.003	1.902	2.112	4.990
0.103	0.001	-0.001	0.879	0.001	1.919	2.096	4.997
0.118	0.000	-0.001	0.873	0.002	1.914	2.099	5.003
0.105	0.000	-0.001	0.881	0.002	1.915	2.097	4.999
0.118	0.000	0.000	0.878	0.001	1.916	2.094	5.006
0.105	-0.001	-0.001	0.880	0.001	1.914	2.099	4.996
0.111	0.000	0.000	0.882	0.001	1.916	2.093	5.004
0.106	-0.001	-0.001	0.880	0.000	1.917	2.096	4.998
0.106	0.001	0.000	0.886	0.000	1.914	2.096	5.000
0.109	0.000	-0.001	0.879	0.000	1.920	2.094	5.000
0.094	-0.001	-0.001	0.895	0.000	1.922	2.088	4.998
0.095	0.001	0.000	0.880	0.000	1.923	2.093	4.994
0.093	0.001	0.000	0.892	0.001	1.929	2.084	4.999
0.090	0.001	-0.001	0.897	0.000	1.932	2.080	4.999

0.085	0.000	-0.001	0.901	0.000	1.937	2.076	4.998
0.077	0.000	-0.001	0.921	0.001	1.942	2.064	5.004
0.069	0.000	-0.001	0.920	0.001	1.954	2.057	5.000
0.064	0.001	0.001	0.920	0.000	1.955	2.057	4.998
0.069	0.000	0.000	0.922	0.002	1.957	2.054	5.002
0.083	0.001	-0.001	0.915	0.001	1.947	2.062	5.007
0.081	0.001	-0.001	0.914	0.000	1.940	2.069	5.002
0.086	0.000	-0.001	0.904	0.000	1.941	2.071	5.001
0.080	0.001	-0.001	0.897	0.000	1.932	2.084	4.991
0.096	-0.001	-0.001	0.889	0.000	1.934	2.082	4.999
0.103	0.000	-0.001	0.888	0.001	1.924	2.087	5.002
0.107	0.001	-0.001	0.880	0.002	1.917	2.095	5.000
0.110	0.000	-0.001	0.871	0.001	1.916	2.100	4.997
0.113	0.001	0.000	0.870	0.001	1.908	2.105	4.998
0.100	0.000	-0.001	0.877	0.001	1.921	2.095	4.994
0.112	-0.001	-0.001	0.885	0.000	1.898	2.107	4.999
0.124	0.001	-0.001	0.861	0.001	1.891	2.121	4.996
0.135	0.001	-0.001	0.861	0.002	1.905	2.106	5.009
0.122	0.001	-0.001	0.866	0.001	1.898	2.113	5.000
0.130	0.001	-0.001	0.859	0.003	1.890	2.120	5.000
0.132	0.001	-0.001	0.853	0.001	1.899	2.116	5.001
0.136	0.001	-0.001	0.854	0.002	1.900	2.113	5.006
0.131	0.001	-0.001	0.858	0.000	1.895	2.118	5.000
0.106	0.001	-0.001	0.879	0.002	1.915	2.097	4.999
0.106	0.001	-0.001	0.874	0.000	1.923	2.094	4.998
0.118	0.001	-0.001	0.870	0.001	1.921	2.095	5.004
0.140	0.001	-0.001	0.833	0.001	1.894	2.128	4.995
0.130	0.001	0.000	0.860	0.001	1.887	2.121	5.002
0.130	0.001	-0.001	0.856	0.001	1.902	2.113	5.002
0.128	0.001	-0.001	0.853	0.001	1.891	2.123	4.996
0.128	0.001	0.000	0.845	0.002	1.891	2.126	4.993
0.134	0.001	-0.001	0.858	0.001	1.893	2.118	5.003
0.127	0.001	-0.001	0.860	0.002	1.886	2.123	4.998
0.125	0.001	-0.001	0.855	0.001	1.895	2.119	4.996
0.140	0.001	0.000	0.862	0.001	1.893	2.114	5.010
0.137	0.001	-0.001	0.852	0.001	1.889	2.122	5.002
0.121	0.001	-0.001	0.867	0.001	1.887	2.121	4.996
0.131	0.001	-0.001	0.866	0.001	1.903	2.106	5.008
0.215	0.002	-0.001	0.772	0.002	1.846	2.175	5.011
0.126	0.001	-0.001	0.856	0.000	1.906	2.111	4.999
0.129	0.001	-0.001	0.863	0.000	1.899	2.113	5.003

0.131	0.001	-0.001	0.871	0.002	1.900	2.105	5.010
0.128	0.001	-0.001	0.858	0.000	1.894	2.118	4.999
0.121	0.001	-0.001	0.864	0.002	1.899	2.113	4.999
0.125	0.002	-0.002	0.865	0.002	1.902	2.109	5.003
0.128	0.001	-0.001	0.866	0.002	1.896	2.112	5.005
0.127	0.001	0.000	0.859	0.001	1.899	2.114	5.001
0.123	0.001	0.000	0.864	0.000	1.891	2.119	4.998
0.122	0.001	-0.001	0.860	0.000	1.903	2.112	4.997
0.137	0.001	-0.001	0.870	0.002	1.895	2.108	5.013
0.136	0.001	-0.001	0.861	0.001	1.893	2.116	5.007
0.126	0.001	-0.002	0.867	0.000	1.892	2.116	5.001
0.123	0.001	-0.001	0.858	0.001	1.896	2.118	4.996
0.128	0.001	-0.001	0.866	0.002	1.891	2.116	5.003
0.122	0.001	0.000	0.865	0.002	1.904	2.108	5.001
0.123	0.002	-0.001	0.866	0.001	1.889	2.120	4.998

015by
Plagioclase

Na	K	Mg	Ca	Fe	Al	Si	Total
0.192	0.001	-0.001	0.794	0.000	1.817	2.191	4.996
0.190	0.001	0.000	0.796	0.000	1.809	2.197	4.994
0.202	0.001	0.000	0.794	0.000	1.822	2.185	5.005
0.181	0.001	-0.001	0.800	0.000	1.810	2.196	4.989
0.200	0.001	-0.001	0.790	0.000	1.814	2.194	4.999
0.182	0.001	-0.001	0.794	0.000	1.816	2.195	4.988
0.186	0.002	-0.001	0.797	0.000	1.812	2.195	4.992
0.207	0.007	-0.001	0.778	0.000	1.806	2.203	5.000
0.178	0.001	-0.001	0.786	0.000	1.820	2.198	4.981
0.172	0.001	-0.001	0.799	0.000	1.806	2.203	4.981
0.176	0.000	-0.001	0.801	0.000	1.825	2.187	4.988
0.181	0.001	-0.001	0.803	0.000	1.800	2.203	4.987
0.182	0.000	0.000	0.787	0.000	1.804	2.208	4.981
0.184	-0.001	0.000	0.801	0.000	1.798	2.206	4.987
0.179	0.001	-0.001	0.786	0.000	1.793	2.218	4.975
0.197	0.001	-0.001	0.789	0.000	1.797	2.209	4.991
0.202	0.001	-0.001	0.782	0.000	1.800	2.209	4.992
0.182	0.000	0.000	0.789	0.000	1.798	2.211	4.980
0.184	0.000	-0.001	0.799	0.000	1.796	2.209	4.985
0.193	0.002	0.000	0.791	0.000	1.800	2.205	4.992
0.228	0.001	-0.001	0.744	0.000	1.757	2.253	4.983

0.221	0.001	0.000	0.751	0.000	1.757	2.251	4.981
0.248	0.006	0.001	0.731	0.000	1.743	2.263	4.993
0.228	0.002	0.000	0.749	0.000	1.751	2.255	4.985
0.217	0.000	-0.001	0.757	0.000	1.753	2.252	4.980
0.231	0.001	0.000	0.744	0.000	1.764	2.246	4.987
0.226	0.001	-0.001	0.744	0.000	1.764	2.248	4.984
0.202	0.001	0.000	0.756	0.000	1.771	2.243	4.974
0.217	0.001	0.000	0.769	0.000	1.776	2.228	4.993
0.204	0.001	-0.001	0.774	0.000	1.773	2.232	4.984
0.099	0.001	0.000	0.870	0.000	1.877	2.132	4.979
0.122	0.001	0.000	0.847	0.000	1.857	2.153	4.980
0.127	0.001	0.000	0.848	0.000	1.865	2.145	4.986
0.126	0.000	-0.001	0.844	0.000	1.860	2.152	4.981
0.133	0.000	0.001	0.837	0.000	1.849	2.162	4.981
0.129	0.000	0.000	0.840	0.000	1.859	2.153	4.981
0.134	0.000	0.000	0.838	0.000	1.846	2.163	4.981
0.161	0.001	0.000	0.834	0.000	1.846	2.158	5.000
0.138	0.000	0.000	0.851	0.000	1.857	2.147	4.994
0.124	0.000	0.001	0.844	0.000	1.854	2.156	4.979
0.142	0.000	0.001	0.845	0.000	1.851	2.154	4.992
0.136	0.001	0.001	0.844	0.000	1.865	2.144	4.992
0.138	0.000	-0.001	0.855	0.000	1.856	2.146	4.995
0.143	0.001	0.000	0.848	0.000	1.851	2.152	4.994
0.153	0.001	0.000	0.833	0.000	1.854	2.155	4.995
0.130	0.001	0.000	0.845	0.000	1.852	2.156	4.983
0.124	0.000	0.000	0.834	0.000	1.853	2.162	4.973
0.141	0.000	0.000	0.838	0.000	1.859	2.151	4.990
0.139	0.000	0.000	0.845	0.000	1.851	2.154	4.990
0.131	0.001	0.000	0.838	0.000	1.852	2.159	4.981
0.133	0.000	0.000	0.852	0.000	1.842	2.159	4.987
0.141	0.000	0.001	0.853	0.000	1.850	2.150	4.995
0.138	-0.001	0.001	0.843	0.000	1.843	2.161	4.986
0.123	0.000	0.001	0.850	0.000	1.847	2.159	4.979
0.127	0.000	0.001	0.847	0.000	1.836	2.167	4.979
0.134	0.000	0.000	0.839	0.000	1.852	2.158	4.983
0.134	0.001	0.001	0.855	0.000	1.842	2.156	4.990
0.124	0.000	-0.001	0.854	0.000	1.840	2.162	4.980
0.138	0.000	0.000	0.845	0.000	1.839	2.164	4.986
0.139	0.000	-0.001	0.833	0.000	1.852	2.160	4.984

004by

Plagioclase

Na	K	Mg	Ca	Fe	Al	Si	Total
0.154	0.002	-0.001	0.828	0.001	1.856	2.155	4.995
0.167	0.002	-0.001	0.821	0.002	1.867	2.147	5.004
0.157	0.001	-0.001	0.833	0.002	1.859	2.149	5.000
0.158	0.002	-0.001	0.823	0.002	1.862	2.152	4.997
0.152	0.002	-0.001	0.823	0.003	1.863	2.153	4.993
0.154	0.002	-0.001	0.824	0.002	1.857	2.155	4.994
0.156	0.001	0.000	0.824	0.002	1.858	2.154	4.995
0.159	0.002	-0.001	0.824	0.003	1.860	2.152	4.999
0.156	0.002	-0.001	0.823	0.002	1.865	2.150	4.997
0.157	0.002	-0.001	0.830	0.003	1.871	2.141	5.002
0.154	0.001	-0.001	0.808	0.002	1.864	2.158	4.987
0.152	0.001	-0.001	0.814	0.002	1.870	2.152	4.990
0.151	0.002	-0.001	0.823	0.003	1.863	2.153	4.993
0.158	0.002	-0.001	0.821	0.001	1.848	2.163	4.993
0.161	0.002	-0.001	0.820	0.003	1.856	2.156	4.998
0.184	0.004	-0.001	0.808	0.003	1.843	2.165	5.007
0.157	0.013	0.000	0.817	0.003	1.851	2.160	4.999
0.158	0.021	0.001	0.795	0.003	1.846	2.171	4.995
0.153	0.004	-0.001	0.822	0.004	1.865	2.149	4.997
0.158	0.003	-0.001	0.820	0.002	1.866	2.150	4.998
0.150	0.001	-0.001	0.827	0.002	1.867	2.148	4.994
0.152	0.001	-0.001	0.834	0.001	1.866	2.145	4.998
0.160	0.001	-0.001	0.809	0.002	1.850	2.168	4.988
0.160	0.002	-0.001	0.824	0.003	1.856	2.155	4.998
0.150	0.001	-0.001	0.814	0.003	1.862	2.158	4.987
0.172	0.001	-0.001	0.816	0.004	1.844	2.164	5.001
0.152	0.002	-0.001	0.816	0.003	1.855	2.161	4.988
0.160	0.002	-0.001	0.811	0.002	1.869	2.152	4.994
0.156	0.001	-0.001	0.832	0.002	1.857	2.151	4.999
0.197	0.002	-0.001	0.791	0.002	1.836	2.178	5.003
0.165	0.002	-0.001	0.818	0.000	1.856	2.157	4.998
0.166	0.002	-0.001	0.826	0.002	1.850	2.157	5.002
0.152	0.002	-0.001	0.819	0.003	1.864	2.153	4.992
0.158	0.002	-0.001	0.824	0.003	1.869	2.145	5.000
0.158	0.003	-0.001	0.822	0.003	1.867	2.147	5.000
0.165	0.003	-0.001	0.823	0.003	1.860	2.151	5.004
0.153	0.002	-0.001	0.822	0.004	1.860	2.154	4.993
0.162	0.002	-0.001	0.820	0.003	1.850	2.160	4.997

0.163	0.002	-0.001	0.825	0.003	1.845	2.162	4.998
0.152	0.002	-0.001	0.821	0.002	1.868	2.150	4.994
0.239	0.001	0.002	0.756	0.002	1.787	2.221	5.006
0.234	0.001	0.002	0.759	0.001	1.779	2.226	5.002
0.264	0.062	0.000	0.647	0.001	1.792	2.251	5.016
0.213	0.047	-0.001	0.684	0.002	1.806	2.238	4.989
0.228	0.001	-0.001	0.756	0.001	1.797	2.217	4.999
0.226	0.001	-0.001	0.755	0.001	1.793	2.221	4.996
0.227	0.001	0.000	0.744	0.002	1.788	2.229	4.991
0.230	0.001	-0.001	0.747	0.001	1.793	2.225	4.994
0.226	0.000	-0.001	0.755	0.001	1.793	2.221	4.995
0.216	0.000	0.000	0.766	0.002	1.802	2.211	4.996
0.348	0.001	-0.001	0.643	0.001	1.676	2.334	5.002
0.333	0.002	0.000	0.644	0.002	1.695	2.323	4.997
0.352	0.001	-0.001	0.637	0.002	1.669	2.341	5.001
0.360	0.001	-0.001	0.627	0.000	1.662	2.350	4.999
0.361	0.002	-0.001	0.618	0.001	1.666	2.351	4.998
0.359	0.002	-0.001	0.617	0.002	1.654	2.360	4.993
0.357	0.001	-0.001	0.620	0.001	1.663	2.353	4.994
0.353	0.002	0.000	0.614	0.000	1.666	2.355	4.989
0.346	0.001	-0.001	0.631	0.001	1.672	2.344	4.994
0.332	0.002	-0.001	0.639	0.002	1.680	2.337	4.990
0.320	0.001	-0.001	0.651	0.002	1.696	2.321	4.991
0.322	0.002	0.000	0.654	0.002	1.703	2.314	4.997
0.341	0.002	-0.001	0.647	0.002	1.689	2.323	5.004
0.326	0.002	-0.001	0.646	0.002	1.691	2.326	4.992
0.334	0.001	-0.001	0.646	0.002	1.690	2.325	4.997
0.321	0.002	-0.001	0.652	0.002	1.689	2.326	4.991
0.322	0.001	0.000	0.648	0.001	1.694	2.324	4.990
0.323	0.001	-0.001	0.647	0.003	1.692	2.326	4.990
0.326	0.002	-0.001	0.663	0.002	1.694	2.316	5.001
0.290	0.001	-0.001	0.677	0.001	1.715	2.302	4.986
0.322	0.002	-0.001	0.648	0.002	1.688	2.329	4.989
0.325	0.002	-0.001	0.636	0.002	1.688	2.333	4.986
0.329	0.001	-0.001	0.649	0.001	1.691	2.324	4.996
0.339	0.002	-0.001	0.652	0.003	1.680	2.328	5.002
0.333	0.002	0.000	0.645	0.001	1.677	2.336	4.993
0.331	0.001	-0.001	0.639	0.001	1.686	2.333	4.990
0.336	0.002	-0.001	0.639	0.002	1.674	2.340	4.991
0.327	0.001	-0.001	0.641	0.002	1.683	2.335	4.987
0.332	0.001	-0.001	0.644	0.002	1.686	2.330	4.994

0.319	0.001	-0.001	0.653	0.002	1.692	2.324	4.991
0.206	0.001	-0.001	0.773	0.001	1.818	2.198	4.997
0.216	0.001	-0.001	0.774	0.000	1.815	2.197	5.004
0.220	0.002	-0.001	0.778	0.000	1.804	2.204	5.006
0.207	0.002	-0.001	0.761	0.000	1.822	2.201	4.992
0.219	0.001	-0.001	0.781	0.000	1.800	2.204	5.006
0.219	0.002	-0.001	0.778	0.002	1.807	2.199	5.007
0.213	0.002	-0.001	0.785	0.001	1.817	2.190	5.008
0.203	0.002	0.000	0.782	0.001	1.813	2.197	4.998
0.220	0.002	-0.001	0.774	0.001	1.817	2.195	5.008
0.207	0.001	0.000	0.778	0.000	1.811	2.201	4.998
0.306	0.002	-0.001	0.676	0.001	1.702	2.307	4.996
0.321	0.002	-0.001	0.666	0.000	1.707	2.306	5.002
0.318	0.002	0.000	0.664	0.001	1.721	2.297	5.003
0.327	0.003	-0.001	0.678	0.000	1.706	2.299	5.013
0.319	0.003	-0.001	0.670	0.001	1.709	2.302	5.004
0.267	0.002	-0.001	0.750	0.000	1.768	2.232	5.019
0.230	0.001	-0.001	0.760	0.001	1.813	2.202	5.007
0.208	0.002	0.000	0.779	0.000	1.818	2.194	5.002
0.211	0.002	-0.001	0.773	0.000	1.811	2.203	4.998
0.209	0.001	-0.001	0.782	0.001	1.832	2.183	5.007
0.196	0.002	-0.001	0.791	0.000	1.839	2.176	5.003
0.200	0.001	0.000	0.787	0.000	1.809	2.199	4.996
0.200	0.001	-0.001	0.796	0.002	1.834	2.175	5.008
0.190	0.001	-0.001	0.802	0.000	1.830	2.178	5.002
0.252	0.001	-0.001	0.768	0.000	1.798	2.205	5.023
0.210	0.001	-0.001	0.786	0.001	1.814	2.194	5.005
0.213	0.002	-0.001	0.786	0.000	1.813	2.194	5.007
0.334	0.002	-0.001	0.674	-0.001	1.689	2.313	5.011
0.190	0.001	-0.001	0.794	-0.001	1.832	2.182	4.998
0.205	0.002	-0.001	0.785	0.000	1.810	2.199	5.000
0.210	0.001	-0.001	0.784	0.000	1.815	2.195	5.004
0.203	0.002	-0.001	0.775	0.001	1.810	2.203	4.994
0.221	0.002	-0.001	0.775	0.002	1.795	2.210	5.004
0.232	0.002	0.000	0.762	0.000	1.780	2.225	5.002
0.230	0.002	-0.001	0.762	0.000	1.797	2.214	5.004
0.219	0.002	-0.001	0.777	0.001	1.800	2.206	5.004
0.228	0.002	-0.001	0.764	0.002	1.801	2.209	5.005
0.234	0.002	-0.001	0.774	0.001	1.805	2.201	5.014
0.218	0.002	-0.001	0.776	0.000	1.815	2.196	5.007
0.270	0.003	-0.001	0.712	0.000	1.748	2.265	4.997

025cy
Hornblende

H	Na	K	Mg	Ca	Fe	Al	Si	Total
2.106	0.376	0.014	3.540	1.797	0.890	1.898	6.820	17.433
2.086	0.376	0.022	3.449	1.783	0.905	2.044	6.742	17.427
2.096	0.360	0.020	3.459	1.789	0.891	2.025	6.765	17.409
2.081	0.337	0.018	3.564	1.808	0.870	1.823	6.872	17.389
2.102	0.347	0.016	3.487	1.782	0.906	1.957	6.792	17.402
2.118	0.351	0.020	3.486	1.763	0.892	1.970	6.805	17.393
2.099	0.355	0.020	3.495	1.781	0.898	1.937	6.802	17.402
2.097	0.353	0.020	3.507	1.784	0.882	1.978	6.778	17.412
2.104	0.369	0.020	3.450	1.768	0.885	1.993	6.800	17.393
2.104	0.370	0.022	3.474	1.790	0.909	2.022	6.742	17.435
2.095	0.383	0.020	3.391	1.790	0.950	2.066	6.716	17.435
2.070	0.390	0.024	3.421	1.797	0.929	2.083	6.712	17.446
2.086	0.410	0.024	3.231	1.816	1.007	2.219	6.648	17.454
2.077	0.390	0.024	3.365	1.808	0.956	2.125	6.672	17.447
2.100	0.386	0.020	3.448	1.798	0.908	2.032	6.740	17.439
2.084	0.363	0.022	3.488	1.814	0.901	1.931	6.795	17.420
2.093	0.369	0.022	3.483	1.797	0.908	1.995	6.750	17.434
2.111	0.363	0.020	3.481	1.801	0.917	1.973	6.779	17.430
2.092	0.320	0.037	3.452	1.811	0.903	1.801	6.917	17.346
2.092	0.376	0.022	3.451	1.797	0.909	2.026	6.737	17.436
2.118	0.404	0.024	3.468	1.771	0.955	2.011	6.741	17.472
2.086	0.421	0.022	3.496	1.748	0.977	2.001	6.717	17.485
2.095	0.402	0.026	3.478	1.767	0.997	1.961	6.750	17.477
2.077	0.436	0.024	3.491	1.784	0.960	1.986	6.719	17.501
2.086	0.421	0.026	3.495	1.734	0.979	1.994	6.733	17.482
2.082	0.437	0.024	3.463	1.758	0.969	1.991	6.734	17.482
2.086	0.435	0.025	3.478	1.768	0.975	1.980	6.742	17.492
2.093	0.431	0.026	3.476	1.760	0.965	1.985	6.761	17.483
2.102	0.436	0.024	3.491	1.766	0.968	2.001	6.727	17.503
2.114	0.330	0.029	3.531	1.828	0.941	1.699	6.940	17.394
2.098	0.385	0.024	3.459	1.777	0.925	2.020	6.754	17.440
2.093	0.397	0.024	3.473	1.796	0.935	2.008	6.731	17.463
2.102	0.395	0.024	3.470	1.789	0.936	2.027	6.729	17.467
2.086	0.397	0.024	3.458	1.781	0.927	2.012	6.750	17.446
2.102	0.384	0.022	3.465	1.777	0.938	2.002	6.755	17.443

2.079	0.394	0.022	3.451	1.787	0.934	2.005	6.750	17.444
2.119	0.393	0.024	3.461	1.811	0.944	2.004	6.740	17.471
2.091	0.388	0.020	3.478	1.776	0.934	1.981	6.757	17.442
2.091	0.383	0.024	3.444	1.804	0.949	2.025	6.728	17.459
2.095	0.388	0.024	3.474	1.785	0.932	2.006	6.752	17.450
2.095	0.372	0.022	3.408	1.775	0.938	2.054	6.744	17.418
2.099	0.381	0.025	3.439	1.766	0.934	2.078	6.722	17.442
2.076	0.389	0.022	3.412	1.781	0.925	2.102	6.703	17.437
2.085	0.377	0.020	3.416	1.795	0.920	2.048	6.747	17.419
2.095	0.387	0.024	3.438	1.782	0.931	2.074	6.711	17.448
2.074	0.383	0.022	3.400	1.782	0.937	2.095	6.716	17.424
2.090	0.384	0.022	3.412	1.776	0.927	2.099	6.721	17.430
2.088	0.386	0.022	3.418	1.796	0.922	2.076	6.722	17.437
2.108	0.377	0.022	3.435	1.782	0.940	2.071	6.724	17.442
2.081	0.396	0.024	3.437	1.780	0.923	2.087	6.709	17.448
2.082	0.360	0.022	3.446	1.782	0.926	1.950	6.816	17.395
2.063	0.378	0.020	3.425	1.788	0.953	2.040	6.730	17.431
2.075	0.374	0.022	3.444	1.800	0.936	1.939	6.799	17.416
2.067	0.374	0.020	3.407	1.806	0.933	2.003	6.762	17.414
2.065	0.369	0.022	3.433	1.787	0.925	2.026	6.746	17.413
2.077	0.351	0.022	3.449	1.779	0.934	1.992	6.769	17.401
2.068	0.353	0.020	3.375	1.826	0.900	2.004	6.797	17.374
2.077	0.367	0.026	3.411	1.753	0.918	2.028	6.773	17.389
2.088	0.366	0.024	3.458	1.805	0.944	1.967	6.755	17.437
2.081	0.391	0.022	3.394	1.817	0.925	2.014	6.756	17.426
2.047	0.373	0.020	3.456	1.789	0.935	1.972	6.753	17.416
2.070	0.374	0.133	3.281	1.685	0.884	2.126	6.771	17.381
2.071	0.364	0.024	3.490	1.789	0.913	1.918	6.802	17.419
2.088	0.350	0.020	3.494	1.810	0.906	1.929	6.785	17.413
2.081	0.339	0.020	3.490	1.802	0.900	1.880	6.830	17.383
2.072	0.339	0.022	3.475	1.786	0.901	1.903	6.821	17.372
2.077	0.337	0.020	3.510	1.796	0.867	1.865	6.857	17.362
2.090	0.359	0.022	3.475	1.804	0.896	1.955	6.789	17.411
2.093	0.348	0.020	3.501	1.795	0.912	1.915	6.796	17.406
2.061	0.350	0.018	3.485	1.771	0.901	1.910	6.821	17.372
2.091	0.331	0.020	3.560	1.788	0.892	1.817	6.870	17.384
2.079	0.314	0.020	3.540	1.795	0.897	1.830	6.882	17.361
2.095	0.328	0.020	3.543	1.791	0.886	1.830	6.869	17.376
2.086	0.326	0.018	3.560	1.794	0.856	1.808	6.890	17.359
2.082	0.343	0.018	3.512	1.810	0.878	1.879	6.834	17.383
2.072	0.339	0.018	3.452	1.749	0.862	1.935	6.861	17.324

2.081	0.342	0.018	3.539	1.792	0.885	1.846	6.845	17.385
2.091	0.340	0.018	3.526	1.804	0.877	1.875	6.835	17.385
2.086	0.362	0.020	3.511	1.782	0.902	1.932	6.796	17.411
2.079	0.354	0.022	3.417	1.784	0.902	1.979	6.804	17.371
2.085	0.354	0.022	3.466	1.792	0.914	1.971	6.780	17.404
2.077	0.362	0.022	3.439	1.800	0.904	1.977	6.790	17.397
2.058	0.343	0.020	3.476	1.811	0.904	1.951	6.788	17.395
2.086	0.345	0.018	3.455	1.791	0.911	1.965	6.784	17.388
2.063	0.336	0.018	3.454	1.803	0.902	1.970	6.787	17.373
2.074	0.341	0.020	3.460	1.792	0.917	1.983	6.771	17.394
2.054	0.381	0.018	3.424	1.814	0.896	2.040	6.737	17.415
2.070	0.392	0.057	3.182	1.710	0.887	2.172	6.816	17.309
2.061	0.368	0.024	3.316	1.764	0.929	2.139	6.719	17.376
2.083	0.385	0.022	3.450	1.815	0.939	2.071	6.680	17.466
2.058	0.359	0.022	3.401	1.788	0.979	1.940	6.825	17.390
2.054	0.377	0.024	3.380	1.798	0.982	2.094	6.694	17.440
2.063	0.379	0.024	3.403	1.801	0.994	2.087	6.681	17.460
2.047	0.369	0.024	3.400	1.815	0.952	2.069	6.702	17.431
2.050	0.375	0.024	3.372	1.796	0.986	2.084	6.702	17.430
2.056	0.374	0.033	3.372	1.810	0.968	2.097	6.697	17.437
2.059	0.399	0.029	3.103	1.694	0.874	2.254	6.815	17.253
2.056	0.375	0.024	3.412	1.815	0.966	2.058	6.709	17.448
2.020	0.362	0.025	3.379	1.817	0.956	2.083	6.695	17.416
2.068	0.370	0.024	3.417	1.809	0.931	2.079	6.712	17.430
2.050	0.400	0.027	3.338	1.784	0.984	2.135	6.682	17.439
2.052	0.400	0.026	3.269	1.744	0.940	2.154	6.760	17.370
2.068	0.374	0.024	3.422	1.802	0.921	2.060	6.737	17.419
2.057	0.389	0.026	3.405	1.792	0.986	2.059	6.705	17.453
2.068	0.387	0.024	3.387	1.770	0.946	2.082	6.733	17.418
2.055	0.401	0.025	3.397	1.752	0.953	2.090	6.723	17.428
2.066	0.386	0.022	3.440	1.799	0.955	2.017	6.750	17.441
2.072	0.384	0.024	3.426	1.773	0.973	2.006	6.757	17.434
2.064	0.329	0.022	3.499	1.813	0.981	1.689	6.953	17.368
2.067	0.226	0.018	3.657	1.844	0.950	1.244	7.240	17.254
2.052	0.382	0.022	3.447	1.799	0.936	2.046	6.716	17.445
2.072	0.388	0.025	3.348	1.727	0.923	2.093	6.770	17.373
2.068	0.375	0.022	3.467	1.765	0.931	2.008	6.774	17.419
2.045	0.360	0.020	3.450	1.781	0.925	2.026	6.757	17.401
2.050	0.370	0.022	3.457	1.789	0.932	2.067	6.714	17.430
2.082	0.373	0.022	3.427	1.794	0.955	2.039	6.742	17.435
2.050	0.363	0.024	3.435	1.769	0.939	2.077	6.720	17.415

2.057	0.334	0.020	3.461	1.798	0.899	2.000	6.787	17.380
2.041	0.352	0.022	3.468	1.742	0.947	1.998	6.778	17.390
2.052	0.356	0.022	3.503	1.685	0.961	2.139	6.680	17.427
2.075	0.278	0.025	3.525	1.827	0.958	1.615	7.016	17.328
2.068	0.369	0.022	3.359	1.811	0.991	1.968	6.799	17.400
2.041	0.352	0.022	3.420	1.796	0.972	1.990	6.776	17.401
2.061	0.335	0.020	3.471	1.807	1.003	1.858	6.841	17.408
2.053	0.346	0.079	3.392	1.666	1.009	2.218	6.639	17.441
2.038	0.344	0.022	3.342	1.818	0.977	1.973	6.799	17.365
2.034	0.349	0.024	3.406	1.809	0.991	1.891	6.830	17.384
2.052	0.361	0.024	3.355	1.811	0.996	2.063	6.716	17.426
2.031	0.344	0.027	3.323	1.837	1.005	2.070	6.718	17.413
2.036	0.359	0.024	3.365	1.799	0.987	2.043	6.745	17.400
2.034	0.374	0.022	3.363	1.789	0.913	2.179	6.674	17.400
2.025	0.363	0.024	3.393	1.788	0.938	2.096	6.699	17.396
2.043	0.371	0.024	3.439	1.787	0.947	2.086	6.679	17.432
2.031	0.380	0.026	3.383	1.783	0.945	2.130	6.670	17.418
2.041	0.377	0.022	3.397	1.799	0.947	2.124	6.658	17.432
2.059	0.367	0.022	3.439	1.794	0.939	2.083	6.688	17.430
2.047	0.363	0.022	3.439	1.772	0.954	2.071	6.707	17.420
2.045	0.363	0.018	3.462	1.782	0.929	2.055	6.714	17.414
2.038	0.373	0.022	3.446	1.765	0.924	2.106	6.686	17.420
2.045	0.368	0.022	3.396	1.765	0.932	2.134	6.689	17.404
2.038	0.422	0.022	3.267	1.756	0.975	2.269	6.603	17.431
2.047	0.397	0.022	3.383	1.760	0.930	2.155	6.674	17.423
2.047	0.408	0.024	3.383	1.769	0.959	2.117	6.674	17.439
2.038	0.397	0.024	3.393	1.744	0.955	2.076	6.725	17.408
2.045	0.377	0.027	3.437	1.758	0.929	2.022	6.751	17.398
2.049	0.391	0.025	3.458	1.740	0.924	2.020	6.753	17.411
2.054	0.372	0.025	3.470	1.750	0.922	2.002	6.763	17.403
2.025	0.387	0.027	3.490	1.743	0.895	1.972	6.786	17.389
2.059	0.363	0.024	3.485	1.751	0.907	1.971	6.785	17.382
2.043	0.365	0.023	3.474	1.766	0.919	1.976	6.762	17.395
2.038	0.366	0.024	3.413	1.791	0.927	2.057	6.728	17.398
2.040	0.359	0.022	3.417	1.791	0.911	2.055	6.726	17.386
2.034	0.369	0.025	3.428	1.787	0.920	2.046	6.716	17.399
2.041	0.375	0.025	3.452	1.788	0.910	2.049	6.714	17.415
2.032	0.383	0.024	3.408	1.784	0.912	2.076	6.709	17.400
2.020	0.380	0.022	3.395	1.795	0.940	2.070	6.696	17.409
2.038	0.382	0.022	3.421	1.792	0.909	2.079	6.711	17.413
2.054	0.380	0.022	3.428	1.798	0.903	2.066	6.723	17.411

2.045	0.372	0.025	3.430	1.803	0.924	2.064	6.705	17.421
2.025	0.369	0.022	3.441	1.766	0.902	2.051	6.733	17.385
2.034	0.386	0.027	3.403	1.765	0.948	2.092	6.688	17.420
2.048	0.389	0.024	3.425	1.761	0.934	2.060	6.715	17.414
2.061	0.377	0.025	3.462	1.748	0.917	2.053	6.724	17.411
2.036	0.386	0.027	3.469	1.759	0.919	2.026	6.722	17.417
2.064	0.380	0.027	3.443	1.759	0.926	2.021	6.749	17.407
2.045	0.392	0.024	3.469	1.745	0.944	2.012	6.729	17.423
2.059	0.393	0.027	3.459	1.744	0.938	2.011	6.740	17.420
2.050	0.393	0.024	3.463	1.760	0.943	2.023	6.719	17.432
2.048	0.397	0.027	3.459	1.730	0.933	2.019	6.750	17.413
2.045	0.383	0.024	3.485	1.760	0.940	2.005	6.726	17.428

015by
Hornblende

H	Na	K	Mg	Ca	Fe	Al	Si	Total
1.968	0.460	0.122	3.214	1.930	1.071	2.174	6.569	17.598
1.968	0.464	0.122	3.207	1.896	1.122	2.139	6.600	17.600
1.959	0.472	0.126	3.199	1.919	1.105	2.170	6.571	17.611
1.971	0.480	0.124	3.216	1.918	1.117	2.163	6.566	17.632
1.970	0.480	0.128	3.204	1.900	1.111	2.143	6.588	17.615
1.975	0.462	0.122	3.238	1.909	1.124	2.139	6.582	17.617
1.982	0.462	0.123	3.246	1.910	1.092	2.139	6.587	17.612
1.975	0.473	0.120	3.197	1.928	1.095	2.156	6.583	17.609
1.978	0.463	0.126	3.204	1.887	1.108	2.217	6.555	17.605
1.973	0.471	0.122	3.180	1.916	1.086	2.224	6.555	17.604
2.008	0.449	0.124	3.220	1.897	1.109	2.153	6.589	17.603
1.996	0.455	0.126	3.258	1.895	1.100	2.117	6.607	17.605
1.991	0.449	0.122	3.238	1.927	1.086	2.109	6.606	17.597
1.991	0.446	0.122	3.252	1.896	1.084	2.116	6.615	17.585
2.000	0.469	0.122	3.243	1.903	1.094	2.115	6.615	17.608
1.970	0.482	0.125	3.194	1.900	1.123	2.196	6.552	17.629
1.950	0.450	0.180	3.076	1.815	1.093	2.351	6.534	17.557
1.973	0.459	0.130	3.139	1.907	1.135	2.257	6.527	17.607
1.996	0.468	0.137	3.143	1.903	1.119	2.258	6.536	17.619
1.992	0.471	0.132	3.132	1.909	1.094	2.255	6.546	17.596
1.977	0.452	0.124	3.370	1.891	1.113	2.161	6.512	17.673
1.984	0.444	0.123	3.364	1.891	1.108	2.176	6.514	17.668
1.954	0.457	0.130	3.357	1.877	1.117	2.177	6.494	17.672
1.972	0.459	0.134	3.348	1.912	1.097	2.185	6.507	17.678

1.979	0.470	0.138	3.326	1.916	1.111	2.187	6.508	17.692
1.968	0.456	0.138	3.351	1.890	1.125	2.190	6.489	17.687
1.965	0.454	0.134	3.336	1.903	1.109	2.187	6.502	17.671
1.965	0.465	0.134	3.357	1.897	1.129	2.209	6.469	17.700
1.972	0.460	0.134	3.336	1.894	1.121	2.208	6.488	17.688
1.940	0.462	0.134	3.315	1.897	1.117	2.221	6.480	17.671
1.972	0.445	0.134	3.336	1.894	1.126	2.284	6.426	17.691
1.984	0.463	0.129	3.308	1.921	1.111	2.260	6.462	17.691
1.975	0.453	0.136	3.318	1.914	1.132	2.248	6.447	17.698
1.996	0.462	0.129	3.315	1.908	1.138	2.240	6.467	17.700
1.993	0.454	0.127	3.310	1.899	1.113	2.246	6.476	17.674
1.979	0.461	0.118	3.298	1.919	1.104	2.237	6.490	17.665
1.982	0.452	0.110	3.342	1.925	1.076	2.211	6.499	17.658
2.017	0.428	0.087	3.428	1.918	1.017	2.078	6.604	17.605
1.994	0.443	0.105	3.370	1.927	1.055	2.194	6.516	17.646
1.998	0.437	0.110	3.375	1.919	1.059	2.180	6.514	17.649

004by
Hornblende

H	Na	K	Mg	Ca	Fe	Al	Si	Total
1.979	0.373	0.199	3.181	1.929	1.386	1.861	6.634	17.654
1.990	0.368	0.192	3.211	1.902	1.405	1.849	6.632	17.659
1.979	0.368	0.194	3.219	1.928	1.405	1.835	6.611	17.673
1.974	0.366	0.187	3.225	1.919	1.397	1.871	6.610	17.666
1.988	0.367	0.191	3.207	1.909	1.408	1.861	6.622	17.665
1.997	0.363	0.192	3.214	1.899	1.420	1.843	6.631	17.662
1.988	0.368	0.195	3.189	1.939	1.387	1.838	6.636	17.663
1.999	0.358	0.193	3.205	1.902	1.390	1.857	6.635	17.652
1.997	0.368	0.195	3.221	1.897	1.418	1.857	6.624	17.675
1.988	0.365	0.193	3.219	1.895	1.389	1.864	6.636	17.653
1.981	0.347	0.202	3.139	1.926	1.414	1.916	6.588	17.650
1.973	0.339	0.187	3.153	1.935	1.402	1.905	6.596	17.633
1.985	0.332	0.184	3.137	1.946	1.366	1.880	6.634	17.602
1.976	0.326	0.183	3.172	1.928	1.400	1.904	6.606	17.625
1.973	0.341	0.190	3.194	1.932	1.374	1.860	6.635	17.629
2.002	0.320	0.173	3.290	1.927	1.327	1.768	6.705	17.606
2.023	0.309	0.170	3.258	1.931	1.337	1.735	6.743	17.581
1.955	0.318	0.184	3.220	1.951	1.369	1.814	6.662	17.607
1.983	0.324	0.193	3.217	1.936	1.361	1.843	6.664	17.619
1.976	0.327	0.194	3.183	1.931	1.394	1.862	6.642	17.624

1.985	0.309	0.147	3.245	1.938	1.385	1.725	6.723	17.570
1.999	0.307	0.166	3.305	1.926	1.402	1.639	6.750	17.597
2.000	0.309	0.153	3.336	1.936	1.351	1.595	6.777	17.573
1.993	0.299	0.144	3.342	1.950	1.384	1.554	6.794	17.574
2.009	0.307	0.149	3.350	1.961	1.351	1.560	6.804	17.581
1.995	0.304	0.149	3.319	1.925	1.368	1.567	6.821	17.552
1.966	0.300	0.148	3.287	1.999	1.350	1.611	6.700	17.566
1.997	0.312	0.151	3.329	1.959	1.380	1.569	6.785	17.591
2.021	0.303	0.151	3.344	1.944	1.367	1.568	6.798	17.583
1.990	0.314	0.156	3.315	1.951	1.371	1.582	6.786	17.578
1.995	0.375	0.219	3.084	1.958	1.522	1.940	6.503	17.729
1.966	0.364	0.216	3.056	1.944	1.527	1.942	6.520	17.692
1.957	0.368	0.212	3.109	1.940	1.493	1.952	6.492	17.700
1.990	0.369	0.216	3.085	1.943	1.512	1.935	6.531	17.703
1.999	0.369	0.211	3.075	1.967	1.506	1.918	6.529	17.706
2.002	0.380	0.201	3.109	1.923	1.480	1.921	6.558	17.685
1.995	0.349	0.201	3.120	1.945	1.485	1.919	6.550	17.683
1.990	0.343	0.197	3.157	1.942	1.460	1.863	6.600	17.661
2.002	0.336	0.183	3.181	1.936	1.456	1.815	6.636	17.644
1.985	0.332	0.181	3.209	1.938	1.426	1.778	6.651	17.626
1.992	0.316	0.166	3.233	1.904	1.337	1.879	6.647	17.583
1.990	0.308	0.163	3.257	1.939	1.353	1.832	6.643	17.598
1.988	0.304	0.159	3.286	1.957	1.327	1.790	6.676	17.589
2.025	0.301	0.166	3.256	1.945	1.320	1.801	6.695	17.579
2.013	0.301	0.155	3.248	1.949	1.277	1.846	6.690	17.557
1.997	0.300	0.154	3.318	1.931	1.320	1.744	6.712	17.576
1.990	0.303	0.152	3.294	1.942	1.341	1.755	6.702	17.577
2.007	0.282	0.146	3.253	1.963	1.305	1.841	6.679	17.558
1.976	0.316	0.172	3.260	1.952	1.337	1.827	6.638	17.606
2.002	0.315	0.166	3.281	1.947	1.311	1.782	6.686	17.590

AUTHOR'S BIOGRAPHY

Calvin was born in Elko, Nevada where he and his family lived for ten years before moving to Ketchikan, Alaska and finally settling in Deerfield, Massachusetts in 2002. In 2008, he graduated from Frontier Regional High School and went on to pursue a degree in Earth Sciences at the University of Maine. At UMaine, Calvin has been an active member of the Catholic Student Association and a proud brother of Sigma Phi Epsilon Fraternity. In his spare time he enjoys playing guitar which has lead him to play for 4 years in the music ministry and the Newman Catholic Center on campus and for 3 years in a folk-bluegrass band. He also enjoys hiking, camping and reading. In the fall, Calvin will pursue a Master's degree in Structural Geology at the University of Massachusetts in Amherst.